Table 1
Antiviral activity against HIV-1 and HIV-2 strains in MT-4 cells

Compound (abbreviation)	EC_{50} (μM)[a]		Selectivity[b]	
	HIV-1_{IIIB}	HIV-2_{EHO}	CC_{50} (μM)[c]	index
2′-Deoxy-4′-C-ethynyl-adenosine (EdA)	0.0095 ± 0.0027[d]	0.006 ± 0.0015	104 ± 6.2	11,000
2′-Deoxy-4′-C-ethynyl-2-fluoroadenosine (EFdA)	0.000073 ± 0.000017	0.000098 ± 0.000022	9.8 ± 3.4	134,000
2′,3′-Dideoxy-4′-C-ethynyl-2-fluoroadenosine (EFddA)	1.17 ± 0.29	1.07 ± 0.23	230 ± 33	196
2′,3′-Didehydro-3′-deoxy-4′-C-ethynyl-2-fluoroadenosine (EFd4A)	0.11 ± 0.033	0.089 ± 0.0007	98 ± 26	899
2′-Deoxy-4′-C-cyano-2-fluoroadenosine (CNFdA)	0.1 ± 0.034	0.09 ± 0.0087	>340	>3,300
2′-Deoxy-4′-C-ethynyl-2-chloroadenosine (ECldA)	0.00069 ± 0.00018	0.0006 ± 0.0000028	230 ± 16	339,000
2′,3′-Dideoxyinosine (ddI)	27 ± 12	24 ± 4.4	>100	>4
3′-Azido-3′-deoxythymidine (AZT)	0.0028 ± 0.00062	0.0022 ± 0.00073	30 ± 7.2	10,800

Anti-HIV activity was determined by the MTT method.
[a] EC_{50} represents the concentration that blocks HIV-1 replication by 50%.
[b] Selectivity index is calculated by the CC_{50}/EC_{50} for HIV-1_{IIIB}.
[c] CC_{50} represents the concentration that suppress the viability of HIV-1-unexposed cells by 50%.
[d] Data shown are mean values with standard deviations for at least three independent experiments.

1RTD, or of tenofovir diphosphate in the ternary complex of HIV-1 RT/DNA/TFV-DP (Tuske et al., 2004).

3. Results

3.1. Antiviral activity of 4′- and 2-substituted deoxyadenosine analogs

We evaluated the activity of 4′- and 2-substituted deoxyadenosine analogs against HIV-1 with the MTT assay using MT-4 cells. The 2′-deoxy-4′-C-ethynyl nucleoside with adenine as the base (EdA) exerted comparable activity to AZT (Table 1). 2-Fluoro substituted EdA, EFdA, was the most potent against HIV-1 with a sub-nanomolar EC_{50} of 0.073 nM. Selectivity of EFdA and ECldA was much increased compared to parental EdA or AZT. However, EFdA was also relatively cytotoxic compared to other inhibitors of this series. The 2-chloro (Cl) substitution also provided enhanced activity but with a decreased toxicity. Further modifications of the sugar ring from 2′-deoxyribose to 2′,3′-dideoxy- or 2′,3′-didehydro-2′,3′-dideoxy-ribose (EFddA or EFd4A) resulted in a drastic decrease of inhibitory potential. Substitution of the 4′-E group with a structurally similar 4′-cyano group also resulted in markedly decreased inhibitory activity. These results indicate that the 3′-OH and 4′-E moieties in the sugar ring are indispensable for high efficacy, and that antiviral activities are augmented by the modification with F- or Cl-moiety at the adenine 2-position. These compounds suppressed the replication of HIV-2 at comparable levels as HIV-1, consistent with the hypothesis that they act as nucleoside reverse transcriptase inhibitors (De Clercq, 1998).

3.2. Antiviral activity against HIV-1 variants resistant to NRTIs

To assess the effect of 4′- and 2-substituted adenosine analogs against drug resistant HIV-1, we generated recombinant infectious clones carrying various NRTI resistant mutations and tested them using the MAGI assay. We found that EdA, EFdA, and ECldA efficiently suppressed many of the viruses resistant to approved NRTI including the multi-drug resistant (MDR) virus, although the 3TC-resistant variant HIV-1_{M184V} and the multi-drug resistant variant HIV-$1_{M41L/T69SSG/T215Y}$ (Winters et al., 1998) showed modestly increased EC_{50} values to these compounds (Table 2). Interestingly, highly active 4′-E analogs, which have 3′-OH such as EFdA or ECldA, were even more effective against the dideoxy-type NRTI resistant variants K65R, L74V, and Q151M complex than they were against WT RT (Table 2). In contrast, 4′-E analogs without 3′-OH (EFddA and EFd4A) were similar or less effective with these resistant variants compared to WT, although the effect seems to be minimal. EFd4A and 2′-deoxy-4′-C-cyano-2-fluoroadenosine (CNFdA) were moderately active against HIV-1_{WT} and HIV-1_{MDR} (Shirasaka et al., 1995), but less active against HIV-1_{M184V}. Susceptibility of even the least active EFddA was still in the low micromolar range, but decreased against both HIV-1_{M184V} and HIV-1_{MDR}, by 84- and 13-fold, respectively.

3.3. Antiviral activity of EFdA against multi-drug resistant clinical isolates

We went on to further characterize EFdA, the most potent compound of the series, against clinical isolates from patients exposed to many anti-AIDS drugs. Five multi-drug resistant strains (HIV-1_{IVR405}, HIV-1_{IVR406}, HIV-1_{IVR412}, HIV-1_{IVR413}, and HIV-1_{A03}), which contained various drug-resistance mutations in HIV-1 genes (Table 3), were used. These clinical isolates showed high resistance to AZT, 3TC (HIV-1_{IVR406}), and ddI (HIV-1_{IVR412}). HIV-1_{IVR415} was also a drug-experienced virus but did not have NRTI-resistance mutations and showed no resistance, or less resistance to the NRTIs tested. Hence, it was used as a drug-sensitive HIV-1. Although antiviral activity of EFdA was slightly reduced against HIV-$1_{IVR405, IVR406, IVR412}$ (5.7- to 7.6-fold) compared to HIV-1_{IVR415}, the activity was high enough to suppress viral replication. It should be emphasized that EFdA was active against HIV-1_{IVR406}, which had the 3TC-resistant M184I substitution.

To evaluate antiviral activity of EFdA to M184V containing isolates in detail, two isolates harboring M184V were used. We used the MAGI assay that directly determines inhibition on a single replication cycle of HIV-1, so that we could eliminate the possible effects of multiple repli-

Table 2
Anti HIV-1 activity against drug-resistant infectious clones

	EC_{50} (μM)[a]								
	EdA	EFdA	EFddA	EFd4A	CNFdA	ECldA	ddI	AZT	3TC
WT	0.021	0.0011	1.2	0.35	0.21	0.0064	4.1	0.015	0.71
K65R	0.0082	0.00023 (×0.2)	1.56	0.2	ND[b]	0.0017 (×0.3)	ND	0.0039 (×0.3)	ND
L74V	0.01	0.00048 (×0.4)	2.52	0.54	ND	0.0015 (×0.2)	14.6	0.019 (×1.3)	ND
V75T	0.0075	0.00067 (×0.6)	9.13	0.95	ND	0.005 (×0.8)	ND	0.047 (×3.1)	ND
M41L/T215Y	0.062	0.0016 (×1.5)	6.7	1.67	ND	0.0065 (×0.1)	ND	0.12 (×8)	ND
M41L/T69SSG/T215Y[c]	0.18	0.0065 (×6)	ND	ND	ND	0.025 (×4)	21	0.20 (×13)	9.9
MDR[d]	0.011	0.00074 (×0.7)	16	0.46	0.69	0.0057 (×0.9)	40	18 (×1200)	1.1
P119S	0.018	0.00067 (×0.6)	ND	ND	ND	0.0062 (×1)	ND	0.0033 (×0.2)	0.6
T165A	0.045	0.001 (×0.9)	ND	ND	ND	0.0082 (×1.3)	ND	ND	0.66
I142V	0.077	0.001 (×0.9)	ND	ND	ND	0.0062 (×1)	ND	0.016 (×1)	0.36
T165R	0.088	0.0016 (×1.5)	ND	ND	ND	0.012 (×1.9)	ND	0.011 (×0.7)	0.28
M184V	0.088	0.0083 (×7.5)	101	6.41	1.76	0.084 (×13)	ND	0.0021 (×0.1)	>100
T165R/M184V	0.6	0.014 (×13)	ND	ND	ND	0.17 (×27)	ND	0.0053 (×0.4)	>100
I142V/T165R/M184V	0.81	0.023 (×22)	ND	ND	ND	0.41 (×65)	ND	0.0076 (×0.5)	>100
T165A/M184V[e]	0.43	0.015 (×14)	ND	ND	ND	0.16 (×25)	ND	0.0049 (×0.3)	>100
P119S/T165A/M184V[e]	0.5	0.015 (×14)	ND	ND	ND	0.20 (×32)	ND	0.0043 (×0.3)	>100

Anti-HIV activity was determined with the MAGI assay.

[a] The data shown are mean values obtained from the results of at least three independent experiments.

[b] ND: not determined.

[c] HIV-1 variant contains T69S substitution and 6-base pair insertions between codons for 69 and 70 (Ser-Gly) with AZT resistant mutations M41L/T215Y (Winters et al., 1998).

[d] Multi-dideoxynucleoside resistant HIV-1 contains mutations (AGT-GGT, SG) in the *pol* region: A62V/V75I/F77L/F116Y/Q151M (Shirasaka et al., 1995).

[e] These variants were reported by Nitanda et al. during induction of Ed4T resistant variants.

cation cycles on measured antiviral activity. In this assay, EFdA effectively suppressed both replication of HIV-1_{IVR443} and HIV-1_{IVR463}. Compared to the EC_{50} value for HIV-1_{WT} in Table 2, reduction of the activity was less than 3-fold, suggesting that EFdA suppresses relatively efficiently 3TC-resistant variants with either M184I or M184V mutations.

3.4. ADA stability of EFdA

Cellular ADA is known to convert dA to dI through deamination. Phosphorylation of the deaminated dA analogs, *e.g.*, dI, is less efficient, resulting in low conversion of the active triphosphate (TP) form. In order to assess if the activation of these compounds to their TP forms would be affected by the activity of ADA, we tested whether ADA can degrade EdA or EFdA. While EdA was almost completely deaminated after 90 min exposure to ADA, EFdA was not deaminated for up to at least 90 min (Fig. 2). These results indicate that the 2-halo-substitution in EdA confers significant resistance to degradation by ADA.

3.5. Phosphorylation of EFdA

Currently available NRTIs need to be converted to the TP form by host cellular kinases before incorporation into newly synthesized proviral DNA. It has been shown that the antiviral effect of NRTIs was reversed by the addition of their physiological counterpart 2′-deoxynucleosides (Bhalla et al., 1990; Mitsuya et al., 1985). To identify the phosphorylation pathway, we examined whether the antiviral activity of EFdA was reversed by the addition of 2′-deoxynucleosides. Surprisingly, the addition of dC decreased the antiviral activity of EFdA in a dose-dependent manner (Fig. 3). In contrast, dT and dG had no effect on the

Table 3
Antiviral activity of EFdA against clinical isolates

Clinical isolates	Amino acid substitutions in the reverse transcriptation	EC_{50} (μM)			
		AZT	ddI	3TC	EFdA
PBMCs[a]					
IVR405	M41L/E44D/D67G/V118I/Q151M/L210W/T215Y	1.76	2.45	0.55	0.0012
IVR406	M41L/E44D/D67N/V118I/M184I/L210W/T215Y/K219R	0.64	1.46	>10	0.0011
IVR412	M41L/E44D/V75L/A98S/L210W/T215F	3.97	9.11	0.83	0.0016
IVR413	M41L/E44D/D67N/V75L/A98S/V118I/L210W/T215Y/K219R	1.0	2.22	1.46	0.00021
A03	M41L/E44D/D67N/L74V/L100I/K103N/V118I/L210W/T215Y	0.53	2.15	0.49	0.0001
IVR415	None	0.0028	0.33	0.078	0.00021
MAGI cells[b]					
IVR443	I135T/Y181C/M184V	0.027	3.6	>100	0.0031
IVR463	M41L/E44D/D67N/M184V/H208Y/L210W/T215Y	0.31	7.5	>100	0.0032

All assays were performed in triplicate. AZT, ddI, and 3TC were served as a control.

[a] Antiviral activity was determined by the inhibition of p24 antigen production in the culture supernatant.

[b] HeLa-CD4/CCR5-LTR/β-gal cells was used for the MAGI assay.

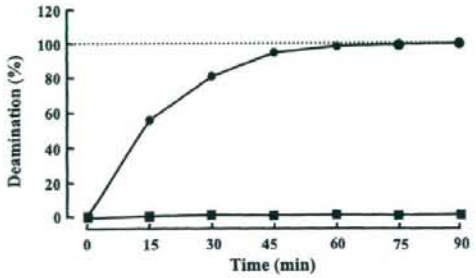

Fig. 2. Stability of EFdA following exposure to ADA. EdA or EFdA was incubated with ADA as described in Section 2. The deamination of adenine to inosine was analyzed by HPLC at indicated time points. The data represent the percent of starting compound (EdA: circle, EFdA: box) that was not deaminated by ADA.

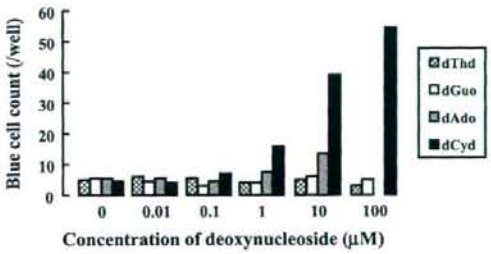

Fig. 3. Reversal of the antiviral activity of EFdA in the presence of 2′-deoxynucleosides. Each 2′-deoxynucleoside was added to the medium with serial dilution in the presence of EFdA (3.5 nM). The effect on EFdA activity was determined by the MAGI assay. An ADA inhibitor, dCF, was used during dA competition.

activity of EFdA. We could observe a slight reversal of the antiviral effect by addition of 10 μM dA with dCF. Effect of 100 μM dA could not be examined because of its cytotoxicity. It should be noted that all other tested analogs, including EFddA and EFd4A, were also reversed by the addition of dC (data not shown).

To confirm that the cellular dCK mediates the phosphorylation of EFdA, we examined the antiviral activity of EFdA in the HT-1080, dCK-deficient HT-1080/Ara-C^r (Obata et al., 2001), and dCK-transduced HT-1080/Ara-C^r cell lines. As expected, the antiviral activity of EFdA was markedly reduced in HT-1080/Ara-C^r cells (677-fold), but restored in dCK-transfected cells (Table 4). The same activity profile was observed with ddC, which is also phosphorylated by dCK (Starnes and Cheng, 1987). In contrast, AZT showed comparable activity among three cell lines, since it is known to be phophorylated mainly by thymidine kinase (Furman et al., 1986). Although dCK appears to be the main enzyme responsible for mono-phosphorylation of EFdA, other kinases, such as adenosine/deoxyadenosine kinases, may be partially involved in mono-phosphorylation of EFdA, especially since weak reduction in antiviral activity of EFdA was observed in addition of dA in high concentrations. Moreover, even in dCK-deficient HT-1080/Ara-C^r cells, EFdA exerted moderate antiviral activity. Hence, while it is possible that other kinases may be contributing to a smaller extent to the phosphorylation of EFdA, it appears that dCK is the enzyme that primarily phosphorylates this inhibitor.

3.6. Resistance to EFdA

In order to elucidate the mechanism of drug resistance to 4′-E analogs, we selected variants resistant to EdA, a parental compound of EFdA with the dose escalating methods (Nameki et al., 2005). After 58 passages in the presence of EdA, the resistant variants were obtained. Sequence analysis of the entire RT region revealed that a novel combination of mutations, I142V/T165R/M184V was introduced. Similar mutations (I119S/T165A/M184V) were observed in a Ed4T-resistant variant (Nitanda et al., 2005). Hence, we generated infectious clones containing these mutations and tested the antiviral activity of 4′-E analogs against them (Table 2). Mutation in T165, either Arg or Ala, enhanced the resistance against EdA, EFdA, and ECldA in the presence of the M184V mutation. Similar resistance profiles were observed for the I142V/M184V mutations. Furthermore, the triple mutant HIV-$1_{I142V/T165R/M184V}$ had the highest resistance among all tested variants. On the other hand, I142V or T165R alone did not affect the antiviral activity of EFdA or ECldA, although EdA or EFddA showed slightly decreased susceptibility. These results suggest that M184V appears to be the main mutation responsible for 4′-E analog resistance, and the addition of I142V and/or T165R augments the effect of M184V.

3.7. Replication of resistant HIV-1

For acquisition of high-level resistance to EFdA as well as EdA, three mutations, I142V, T165R, and M184V were required as described above. To examine the effect of the mutations on the viral replication kinetics we performed an assay that follows production of p24 gag antigen. All clones with M184V showed reduced replication kinetics (Fig. 4A), consistent with the reports that introduction of M184V markedly impairs replication kinetics (Wainberg et al., 1996; Yoshimura et al., 1999). Introduc-

Table 4
The effect of dCK expression on the EFdA antiviral activity[a]

Cell	EC_{50} (μM)[b]		
	AZT	ddC	EFdA
HT-1080	0.0032 ± 0.001	0.75 ± 0.22	0.00031 ± 0.0001
HT-1080/Ara-C^r	0.0027 ± 0.0005 (0.84)	84 ± 15 (112)	0.21 ± 0.03 (677)
HT-1080/Ara-C^r/dCK	0.0025 ± 0.00074 (0.78)	0.51 ± 0.16 (0.68)	0.000098 ± 0.000034 (0.32)

[a] SEAP activity in the culture supernatants were determined on day 2 after virus infection.
[b] The data shown are mean ± S.D. and fold increase in EC_{50} compared to HT-1080 is shown in parentheses.

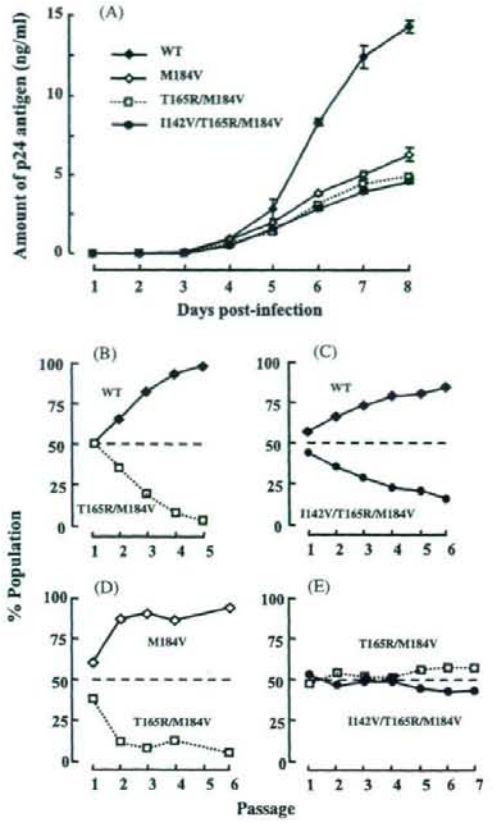

Fig. 4. Replication kinetics of HIV-1 clones with mutations. Production of p24 antigen in culture supernatant was determined with a commercially available p24 antigen kit. Profiles of replication kinetics (p24 production) of HIV-1_{WT} (closed diamonds), HIV-1_{M184V} (open diamonds), HIV-$1_{T165R/M184V}$ (open squares with broken line) and HIV-$1_{I142V/T165R/M184V}$ (open circles) were determined with MT-2 (A). Representative results from three independent triplicate determinations of p24 production with newly titrated viruses are shown. MT-2 cells were infected simultaneously with equal amounts of two HIV-1 clones to be compared. At each passage (5–6 days) the proviral sequences were determined and the percent population of each clone is reported at different passage; competition of WT and T165R/M184V (B); competition of WT with I142V/T165R/M184V (C); competition of M184V with T165R/M184V (D), and competition of T165R/M184V with I142V/T165R/M184V (E). At least two independent CHRAs were performed and are shown the representative results.

tion of T165R or I142V/T165R mutations in an M184V background (HIV-$1_{T165R/M184V}$ or HIV-$1_{I142V/T165R/M184V}$, respectively) further impaired HIV replication compared to HIV-1_{M184V}. I142V which enhanced EFdA resistance of HIV-$1_{T165R/M184V}$ (Table 2) conferred no replication rescue of HIV-$1_{T165R/M184V}$. To determine detailed replication kinetics, we performed CHRA which compares qualitatively viral replication. As shown in Fig. 4A, HIV-$1_{T165R/M184V}$ and HIV-$1_{I142V/T165R/M184V}$ showed reduced replication kinetics compared to HIV-1_{WT} (Fig. 4B and C). Replication kinetics ofHIV-$1_{I142V/T165R/M184V}$ was comparable to that of HIV-$1_{T165R/M184V}$, which showed further reduced replication kinetics compared to HIV-1_{M184V} (Fig. 4D and E). In another experiment, replication of HIV-$1_{I142V/T165R/M184V}$ was slightly decreased compared to HIV-$1_{T165R/M184V}$ (data not shown). These results suggest that introduction of three EdA mutations that also confers EFdA resistance impaired replication of HIV-1 in much greater extent compared to that of M184V.

4. Discussion

At present, HIV-1 variants containing NRTI-resistance mutations are widely observed not only in NRTI-experienced but also in NRTI-naïve patients. In such cases treatment failure is sometimes observed within short periods. The NRTI tenofovir, appears to be more effective against drug-experienced HIV-1 strains (Srinivas and Fridland, 1998). Unlike the other clinically available NRTIs, tenofovir has highly flexible acyclic ribose ring without a 3′-OH. Structural studies have suggested that the compact size of this inhibitor may contribute to the absence of highly resistant mutant strains against tenofovir (Tuske et al., 2004). Despite its unique structural profile, tenofovir is similar to other NRTIs in that it also lacks a 3′-OH group.

In contrast, the highly active 4′-E analogs such as EFdA retain the 3′-OH group of the canonical dNTP substrate. Similar to other NRTIs, they are also phosphorylated by cellular enzymes to their TP active form, which in turn serves as a substrate for HIV RT that incorporates them in an elongating primer during DNA synthesis. Following incorporation, replication is further inhibited by chain termination, although the specific mechanism of chain termination remains to be elucidated. Despite the fact that the 4′-E analogs have a 3′-OH like canonical dNTP substrates, cellular polymerases are likely to discriminate against these analogs, and not incorporate them during cellular DNA polymerization, as suggested by *in vitro* experiments with mitochondrial polymerase γ (Nakata et al., 2007). Alternatively, it is also possible that cellular proofreading systems excise the 4′-E analogs after their incorporation into cellular DNA.

The 3′-OH also plays an important role in phosphorylation of EdA analogs. Based on crystallographic results Sabini et al. reported that the interaction between 3′-OH of nucleosides and catalytic site of dCK was important for efficient nucleoside phosphorylation (Sabini et al., 2003). Alternatively, it is possible that the EFddA and EFd4A nucleosides that lack 3′-OH are poor substrates for HIV RT. The substitution at the 2-position of the purine base is also likely to contribute to highly potent *in vivo* activity of EF- or ECldA, possibly by preventing deamination of the inhibitor by ADA. ADA deaminates the adenine base into inosine, which is a poor substrate for cellular kinases. Similar ADA resistance has been reported for 2′-deoxy-2-chloroadenosine, a chemotherapeutic agent against hairy cell leukemia and chronic lymphocytic leukemia (Carson et al., 1980). ADA resistance may contribute to a longer intracellular half-life for EFdA-TP as compared to that of AZT (Nakata et al., 2007), indicating that substitution of 2-position plays an important role in sustained activity. When CEM cells were exposed to AZT or EFdA at concen-

tration of 0.1 μM, amounts of corresponding intracellular TP-forms were comparable (Nakata et al., 2007). However, inhibitory effect of EFdA in MT-4 and MAGI cells was approximately 40- and 15-fold superior compared to that of AZT (Tables 1 and 2). Taken together, HIV-1 RT appears to preferentially incorporate EFdA-TP compared to AZT-TP, although detailed enzymatic confirmation is needed. The parental EdA also seems to be a good substrate for HIV-1 RT; however, it may be subjected to deamination, resulting in comparable activity to AZT.

There are at least two mechanisms by which HIV RT can become resistant to NRTIs: first, HIV RT can acquire mutations at, or close to the dNTP-binding site, such that help it discriminate against NRTI-triphosphates, while it retains its ability to recognize the normal dNTP substrates (Huang et al., 1998). In the case of M184V/I the discrimination is based on steric conflict between a part of the inhibitor (the sulfur atom of the thioxolane ring in the case of 3TC), and the β-branched side chain of Val or Ile at the mutation site (Sarafianos et al., 1999). Mutations at other residues of the dNTP-binding site are responsible for discrimination of dideoxynucleosides from dNTPs during both the substrate-recognition (Martin et al., 1993) and the catalytic steps (Deval et al., 2002; Selmi et al., 2001). The other mechanism of NRTI resistance is based on an excision reaction (phosphorolysis) that unblocks NRTI-terminated primers using a molecule of ATP as the pyrophosphate donor (Meyer et al., 1999). The product of this reaction is a dinucleoside tetraphosphate and an unblocked primer that can continue viral DNA synthesis. In this case, the role of resistance mutations is to optimize binding of an ATP molecule that is used for the nucleophilic attack at the primer terminus. Most of AZT resistance as well as multi-NRTI resistance of RT with insertions at the fingers subdomain are thought to be based on an ATP-based unblocking mechanism. The insertions in RT destabilize the normally stable ternary complex (RT/template-primer/dNTP) and facilitate the ATP-mediated pyrophospholysis (Boyer et al., 2002). The fingers insertion mutant can excise all nucleotide analogs, with various degrees of efficiency.

Our molecular modeling studies are consistent with a mechanism of resistance to 4′-E analogs that involves steric hindrance between the 4′-E group of the inhibitors and the side chain of V184, reminiscent of the resistance mechanism to 3TC. While a single M184V mutation confers strong resistance to 3TC (>100-fold), it causes only moderate (8- to 13-fold) resistance to EFdA and ECldA (Table 2). This is consistent with our molecular modeling analysis where the bulky and rigid 4′-E moiety appears to cause some steric hindrance with the Val or Ile side chain at position 184 during incorporation of the 4′-E nucleotides by the M184V enzyme (Fig. 5). The steric interaction appears to be stronger during incorporation of 3TC-TP (Fig. 5E) than EFdA-TP (Fig. 5C). Interestingly, the M184V mutation appears to confer stronger resistance to 4′-methyl substituted nucleotides, than to the 4′-ethynyl substituted nucleotides (Kodama et al., 2001). The decreased resistance of 4′-ethynyl substituted compounds may be in part the result of compensatory favorable interactions of the longer ethynyl group with residues of the dNTP binding site, including Y115 and D185. Such interactions may moderate the effect of the steric interactions of the 4′-ethynyl with residue V184 in the M184V mutant. Resistance of M184V to dideoxy-derivatives such as EFddA was unexpectedly high (84-fold). Although we cannot explain the detailed mechanism of the difference in resistance, it is possible that the presence of a 3′-OH in the EFdA (but not in the EFddA and EFd4A) results in more stabilizing interactions with residues such as Q151 that compensate for the steric hindrance by M184V (Fig. 5D). Hence, EFddA and EFd4A may be easier to push out of the binding pocket than analogs with a 3′-OH. For stronger resistance to 4′-E-2-halo-dAs, other mutations at positions 142 and 165 in addition to the M184V are required (Table 2) to substantially decrease inhibitor binding. It should be noted that the T165R/M184V mutations were also observed during induction of resistant variants to parental compound EdA. Nitanda et al. also reported that resistant variants for 4′-Ed4T contain M184V with T165A (Nitanda et al., 2005). As shown in Fig. 5A, the effect of the T165R mutation seems to be through the loss of a hydrogen bond between the side chain of Q182 and the side chain OH moiety of T165. Instead, there may be a hydrogen bond between C=O of the main chain of 184 and Q182 in the case of T165R/A, which would affect the positioning of the residue in position 184. Interestingly, HIV-2 has an Arg residue at position 165, whereas HIV-1 has Thr. We could not find decreased susceptibility in HIV-1_{T165R} or HIV-2, indicating that R165 becomes relevant only when Val is at the 184 position. When this residue is Met (T165R in M184 background), resistance is not affected substantially (1.5- to 2-fold resistance, Table 2) because of the flexibility of the Met side chain. However, when the 184 residue is Val (T165R/M184V), the position of 184 may be affected in a way that exacerbates the steric interactions between the ethynyl group of the incoming EFdA and the side chain of V184, resulting in resistance to EFdA and the other 4′-E analogs (13–27-fold resistance, Table 2). At this point it is not clear why the I142V mutation further augmented the effects of M184V and T165R. Finally, as shown in Fig. 5B, there are no apparent substantial steric problems for binding of EFdA to HIV-$1_{M41L/T69SSG/T215Y}$ RT, and the enzyme–inhibitor interactions are likely to be similar to those with dNTP and consistent with the relatively low resistance observed with this variant (Table 2) that is known to cause strong excision-based NRTI resistance. Crystallographic studies with the RT resistant variants complexed with the inhibitors should provide more insights into the mechanism of resistance.

The M184V, one of three mutations associated with EFdA resistance, develops rapidly under therapy with 3TC and has been reported to alter several profiles of RT function, including decreased RT processivity (Back et al., 1996), reduced nucleotide-dependent primer unblocking (Gotte et al., 2000), and increased fidelity (Wainberg et al., 1996). These profiles result in impaired viral fitness, hypersensitivity to other NRTIs, especially AZT (Larder et al., 1995), and delayed appearance of mutations, respectively. Our results show that modest resistance to EdA comes at a significant cost for the virus: The I142V and T165R mutations reduced even further viral replication kinetics of M184V-containing virus. Furthermore, the virus containing these mutations retains the AZT hyper-susceptibility which is induced by

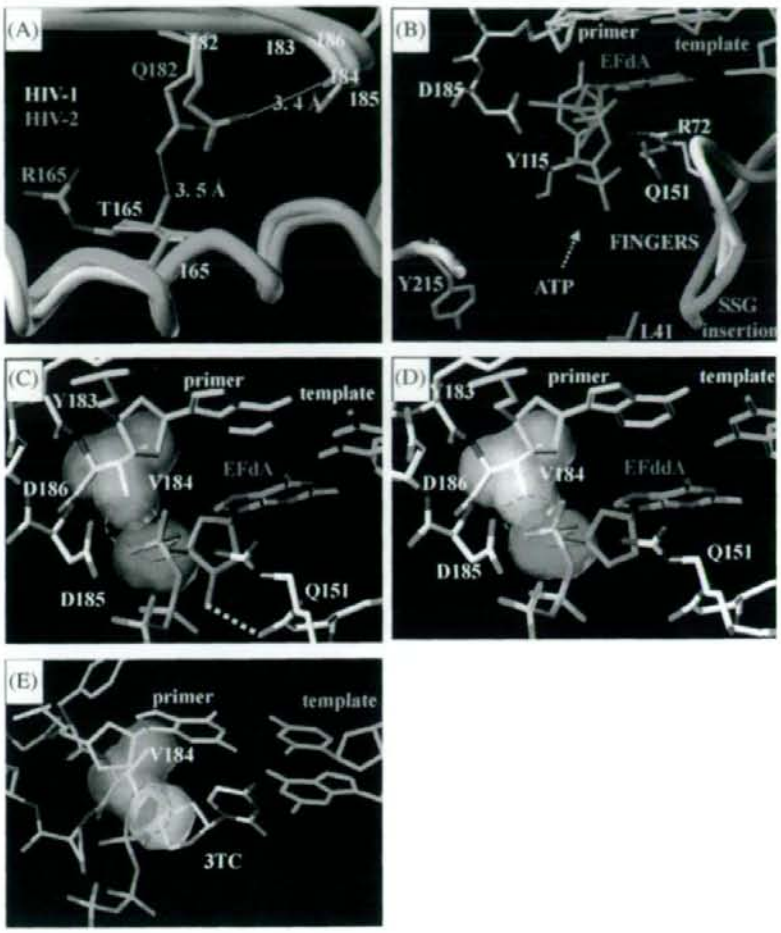

Fig. 5. Structural modeling of reverse transcriptase and compounds. (A) Superposition of the polymerase active sites of HIV-1 (gray) and HIV-2 (magenta) reverse transcriptases. Q182 makes a hydrogen bond with T165 in HIV-1. In the T165R mutant of HIV-1, the arginine side chain is expected to have a conformation similar to the one observed for R165 in HIV-2. In this context, Arg does not make a hydrogen bond with the side chain of residue 182 that may now interact with the main chain carbonyl of M184, which is at the immediate vicinity of the inhibitor-binding site. Such interaction may explain how the T165R mutation exacerbates the role of the M184V mutation in resistance to EFdA. (B) Proposed interactions of EFdA-triphosphate (TP) at the polymerase active site of the "fingers-insertion" NRTI-resistant HIV-1 RT, carrying the M41L/T69SSG/T215Y mutations. Possible steric interactions between the 4′-E group of EFdA-TP (C) or EFddA-TP (D) and the sulfur (S) of the pseudosugar ring of 3TC-TP (E). Van der Waals surfaces of 4′-E group (C and D) and S at sugar ring (E) are indicated in green and yellow. Possible steric interactions are shown as overalap of Van der Waal volumes of interacting atoms (in red).

M184V (Table 2), although further experiments are needed. These results suggest that the I142V and T165R mutations simply enhance resistance of M184V RT to EdA rather than optimize the viral fitness of the M184V virus. The increased cost for the virus to overcome inhibition pressure by EdA may have significant clinical benefits in the treatment of HIV infections.

Since EFdA is initially phosphorylated mainly by dCK and its activity was attenuated by addition of dC (data not shown), it is likely that dC analogs, such as 3TC and emtricitabine (FTC) that are mainly phosphorylated by dCK would act as a competitor of EFdA phosphorylation. However, one of dC analogs, apricitabine (ATC) showed little competition for the intracellular phosphorylation of 3TC and FTC (Bethell et al., 2007). Thus, interaction of NRTIs using identical phosphorylation enzymes should be carefully examined.

In conclusion, we have shown that the 2-halogen substituted EdAs have exceptionally potent subnanomolar antiviral activities. The 2-F substituted analog exhibited the highest potency and had a selectivity index significantly improved over that of approved NRTIs. In fact, results from our parallel studies with mice show no toxicity of EFdA (data not shown). The earlier studies also showed that a

parental nucleoside, EdA was not toxic in mice (Kohgo et al., 2004). The half-life of the intracellular TP form of EFdA is substantially extended (~17 h) compared to that of AZT (~3 h) (Nakata et al., 2007), suggesting that it may be possible to administer these inhibitors once a day. Further investigation may lead to their development as potential therapeutics against HIV infections.

Acknowledgements

We would like to thank S. Oka, T. Sasaki, M. Emerman, J. Overbaugh, K.-T. Jeang, M. Baba for providing HIV-1 clinical isolates, HT-1080 and HT-1080/Ara-C^r cell lines, HeLa-CD4-LTR/β-gal cells and HeLa-CD4/CCR5-LTR/β-gal cells through the AIDS Research and Reference Reagent Program, Division of AIDS, National Institute of Allergy and Infectious Diseases (Bethesda, MD), pNL101, pLTR-SEAP-puro, respectively. A.K. is supported by the 21st Century COE program of the ministry of Education, Culture, Sports, Science, and Technology. This work was supported by a grant for the promotion of AIDS Research from the Ministry of Health, Labor, and Welfare (E.K. and M.M.), a grant for Research for Health Sciences Focusing on Drug Innovation from The Japan Health Sciences Foundation (E.K. and M.M.).

References

Back NK, Nijhuis M, Keulen W, Boucher CA, Oude Essink BO, van Kuilenburg AB, et al. Reduced replication of 3TC-resistant HIV-1 variants in primary cells due to a processivity defect of the reverse transcriptase enzyme. EMBO J 1996;15(15):4040–9.

Bethell R, De Muys J, Lippens J, Richard A, Hamelin B, Ren C, et al. In vitro interactions between apricitabine and other deoxycytidine analogues. Antimicrob Agents Chemother 2007;51(8):2948–53.

Bhalla KN, Li GR, Grant S, Cole JT, MacLaughlin WW, Volsky DJ. The effect in vitro of 2′-deoxycytidine on the metabolism and cytotoxicity of 2′,3′-dideoxycytidine. AIDS 1990;4(5):427–31.

Boyer PL, Sarafianos SG, Arnold E, Hughes SH. Nucleoside analog resistance caused by insertions in the fingers of human immunodeficiency virus type 1 reverse transcriptase involves ATP-mediated excision. J Virol 2002;76(18):9143–51.

Carson DA, Wasson DB, Kaye J, Ullman B, Martin Jr DW, Robins RK, et al. Deoxycytidine kinase-mediated toxicity of deoxyadenosine analogs toward malignant human lymphoblasts in vitro and toward murine L1210 leukemia in vivo. Proc Natl Acad Sci USA 1980;77(11):6865–9.

De Clercq E. The role of non-nucleoside reverse transcriptase inhibitors (NNRTIs) in the therapy of HIV-1 infection. Antiviral Res 1998;38(3):153–79.

Deval J, Selmi B, Boretto J, Egloff MP, Guerreiro C, Sarfati S, et al. The molecular mechanism of multidrug resistance by the Q151M human immunodeficiency virus type 1 reverse transcriptase and its suppression using alpha-boranophosphate nucleotide analogues. J Biol Chem 2002;277(44):42097–104.

Dutschman GE, Grill SP, Gullen EA, Haraguchi K, Takeda S, Tanaka H, et al. Novel 4′-substituted stavudine analog with improved anti-human immunodeficiency virus activity and decreased cytotoxicity. Antimicrob Agents Chemother 2004;48(5):1640–6.

Furman PA, Fyfe JA, St Clair MH, Weinhold K, Rideout JL, Freeman GA, et al. Phosphorylation of 3′-azido-3′-deoxythymidine and selective interaction of the 5′-triphosphate with human immunodeficiency virus reverse transcriptase. Proc Natl Acad Sci USA 1986;83(21):8333–7.

Gotte M, Arion D, Parniak MA, Wainberg MA. The M184V mutation in the reverse transcriptase of human immunodeficiency virus type 1 impairs rescue of chain-terminated DNA synthesis. J Virol 2000;74(8):3579–85.

Haraguchi K, Takeda S, Tanaka H, Nitanda T, Baba M, Dutschman GE, et al. Synthesis of a highly active new anti-HIV agent 2′,3′-didehydro-3′-deoxy-4′-ethynylthymidine. Bioorg Med Chem Lett 2003;13(21):3775–7.

Huang H, Chopra R, Verdine GL, Harrison SC. Structure of a covalently trapped catalytic complex of HIV-1 reverse transcriptase: implications for drug resistance. Science 1998;282(5394):1669–75.

Jeang KT, Chun R, Lin NH, Gatignol A, Glabe CG, Fan H. In vitro and in vivo binding of human immunodeficiency virus type 1 Tat protein and Sp1 transcription factor. J Virol 1993;67(10):6224–33.

Kajiwara K, Kodama E, Matsuoka M. A novel colorimetric assay for CXCR4 and CCR5 tropic human immunodeficiency viruses. Antivir Chem Chemother 2006;17(4):215–23.

Kimpton J, Emerman M. Detection of replication-competent and pseudotyped human immunodeficiency virus with a sensitive cell line on the basis of activation of an integrated beta-galactosidase gene. J Virol 1992;66(4):2232–9.

Kodama EI, Kohgo S, Kitano K, Machida H, Gatanaga H, Shigeta S, et al. 4′-Ethynyl nucleoside analogs: potent inhibitors of multidrug-resistant human immunodeficiency virus variants in vitro. Antimicrob Agents Chemother 2001;45(5):1539–46.

Kohgo S, Yamada K, Kitano K, Iwai Y, Sakata S, Ashida N, et al. Design, efficient synthesis, and anti-HIV activity of 4′-C-cyano- and 4′-C-ethynyl-2′-deoxy purine nucleosides. Nucleosides Nucleotides Nucleic Acids 2004;23(4):671–90.

Kosalaraksa P, Kavlick MF, Maroun V, Le R, Mitsuya H. Comparative fitness of multi-dideoxynucleoside-resistant human immunodeficiency virus type 1 (HIV-1) in an In vitro competitive HIV-1 replication assay. J Virol 1999;73(7):5356–63.

Larder BA, Kemp SD, Harrigan PR. Potential mechanism for sustained antiretroviral efficacy of AZT-3TC combination therapy. Science 1995;269(5224):696–9.

Little SJ, Holte S, Routy JP, Daar ES, Markowitz M, Collier AC, et al. Antiretroviral-drug resistance among patients recently infected with HIV. N Engl J Med 2002;347(6):385–94.

Martin JL, Wilson JE, Haynes RL, Furman PA. Mechanism of resistance of human immunodeficiency virus type 1 to 2′,3′-dideoxyinosine. Proc Natl Acad Sci USA 1993;90(13):6135–9.

Meyer PR, Matsuura SE, Mian AM, So AG, Scott WA. A mechanism of AZT resistance: an increase in nucleotide-dependent primer unblocking by mutant HIV-1 reverse transcriptase. Mol Cell 1999;4(1):35–43.

Mitsuya H, Weinhold KJ, Furman PA, St Clair MH, Lehrman SN, Gallo RC, et al. 3′-Azido-3′-deoxythymidine (BW A509U): an antiviral agent that inhibits the infectivity and cytopathic effect of human T-lymphotropic virus type III/lymphadenopathy-associated virus in vitro. Proc Natl Acad Sci USA 1985;82(20):7096–100.

Miyake H, Iizawa Y, Baba M. Novel reporter T-cell line highly susceptible to both CCR5- and CXCR4-using human immunodeficiency virus type 1 and its application to drug susceptibility tests. J Clin Microbiol 2003;41(6):2515–21.

Nakata H, Amano M, Koh Y, Kodama E, Yang G, Bailey CM, et al. Activity against Human Immunodeficiency Virus Type 1, intracellular metabolism, and effects on human DNA polymerases of 4′-ethynyl-2-fluoro-2′-deoxyadenosine. Antimicrob Agents Chemother 2007;51(8):2701–8.

Nameki D, Kodama E, Ikeuchi M, Mabuchi N, Otaka A, Tamamura H, et al. Mutations conferring resistance to human immunodeficiency virus type 1 fusion inhibitors are restricted by gp41 and Rev-responsive element functions. J Virol 2005;79(2):764–70.

Nitanda T, Wang X, Kumamoto H, Haraguchi K, Tanaka H, Cheng YC, et al. Anti-human immunodeficiency virus type 1 activity and resistance profile of 2′,3′-didehydro-3′-deoxy-4′-ethynylthymidine in vitro. Antimicrob Agents Chemother 2005;49(8):3355–60.

Obata T, Endo Y, Tanaka M, Uchida H, Matsuda A, Sasaki T. Deletion mutants of human deoxycytidine kinase mRNA in cells resistant to antitumor cytosine nucleosides. Jpn J Cancer Res 2001;92(7):793–8.

Ohrui H. 2′-Deoxy-4′-C-ethynyl-2-fluoroadenosine, a nucleoside reverse transcriptase inhibitor, is highly potent against all human immunodeficiency viruses type 1 and has low toxicity. Chem Rec 2006;6(3):133–43.

Palella Jr FJ, Delaney KM, Moorman AC, Loveless MO, Fuhrer J, Satten GA, et al. Declining morbidity and mortality among patients with advanced human immunodeficiency virus infection. HIV Outpatient Study Investigators. N Engl J Med 1998;338(13):853–60.

Sabini E, Ort S, Monnerjahn C, Konrad M, Lavie A. Structure of human dCK suggests strategies to improve anticancer and antiviral therapy. Nat Struct Biol 2003;10(7):513–9.

Sarafianos SG, Das K, Clark Jr AD, Ding J, Boyer PL, Hughes SH, et al. Lamivudine (3TC) resistance in HIV-1 reverse transcriptase involves steric hindrance with beta-branched amino acids. Proc Natl Acad Sci USA 1999;96(18):10027–32.

Selmi B, Boretto J, Sarfati SR, Guerreiro C, Canard B. Mechanism-based suppression of dideoxynucleotide resistance by K65R human

immunodeficiency virus reverse transcriptase using an alpha-boranophosphate nucleoside analogue. J Biol Chem 2001;276(51):48466–72.

Shirasaka T, Kavlick MF, Ueno T, Gao WY, Kojima E, Alcaide ML, et al. Emergence of human immunodeficiency virus type 1 variants with resistance to multiple dideoxynucleosides in patients receiving therapy with dideoxynucleosides. Proc Natl Acad Sci USA 1995;92(6):2398–402.

Srinivas RV, Fridland A. Antiviral activities of 9-*R*-2-phosphonomethoxypropyl adenine (PMPA) and bis(isopropyloxymethylcarbonyl)PMPA against various drug-resistant human immunodeficiency virus strains. Antimicrob Agents Chemother 1998;42(6):1484–7.

Starnes MC, Cheng YC. Cellular metabolism of 2′,3′-dideoxycytidine, a compound active against human immunodeficiency virus in vitro. J Biol Chem 1987;262(3):988–91.

Tuske S, Sarafianos SG, Clark Jr AD, Ding J, Naeger LK, White KL, et al. Structures of HIV-1 RT-DNA complexes before and after incorporation of the anti-AIDS drug tenofovir. Nat Struct Mol Biol 2004;11(5):469–74.

Wainberg MA, Drosopoulos WC, Salomon H, Hsu M, Borkow G, Parniak M, et al. Enhanced fidelity of 3TC-selected mutant HIV-1 reverse transcriptase. Science 1996;271(5253):1282–5.

Weiner MP, Costa GL, Schoettlin W, Cline J, Mathur E, Bauer JC. Site-directed mutagenesis of double-stranded DNA by the polymerase chain reaction. Gene 1994;151(1–2):119–23.

Winters MA, Coolley KL, Girard YA, Levee DJ, Hamdan H, Shafer RW, et al. A 6-basepair insert in the reverse transcriptase gene of human immunodeficiency virus type 1 confers resistance to multiple nucleoside inhibitors. J Clin Invest 1998;102(10):1769–75.

Yoshimura K, Feldman R, Kodama E, Kavlick MF, Qiu YL, Zemlicka J, et al. In vitro induction of human immunodeficiency virus type 1 variants resistant to phosphoralaninate prodrugs of *Z*-methylenecyclopropane nucleoside analogues. Antimicrob Agents Chemother 1999;43(10):2479–83.

Bioorganic & Medicinal Chemistry 16 (2008) 9184–9187

Contents lists available at ScienceDirect

Bioorganic & Medicinal Chemistry

journal homepage: www.elsevier.com/locate/bmc

Identification of minimal sequence for HIV-1 fusion inhibitors

Hiroki Nishikawa [a], Shinya Oishi [a], Mizuno Fujita [a], Kentaro Watanabe [a], Rei Tokiwa [a], Hiroaki Ohno [a], Eiichi Kodama [b], Kazuki Izumi [b], Keiko Kajiwara [b], Takeshi Naitoh [b], Masao Matsuoka [b], Akira Otaka [a,c], Nobutaka Fujii [a,*]

[a] Graduate School of Pharmaceutical Sciences, Kyoto University, Sakyo-ku, Kyoto 606-8501, Japan
[b] Laboratory of Virus Control, Institute for Virus Research, Kyoto University, Sakyo-ku, Kyoto 606-8507, Japan
[c] Graduate School of Pharmaceutical Sciences, The University of Tokushima, Tokushima 770-8505, Japan

ARTICLE INFO

Article history:
Received 7 August 2008
Revised 29 August 2008
Accepted 5 September 2008
Available online 10 September 2008

Keywords:
HIV-1
Fusion inhibitor
α-Helix
Heptad repeat

ABSTRACT

Emergence of multi-drug resistant HIV-1 is a serious problem for AIDS treatment. Recently, the virus-cell membrane fusion process has been identified as a promising target for the development of novel drugs against these resistant variants. In this study, we identified a 29-residue peptide fusion inhibitor, SC29EK, which shows activity comparable to the previously reported inhibitor SC35EK. Some residues in SC29EK not required for interaction with virus gp41 heptad repeat 1 (HR1) were replaced with a non-proteinogenic amino acid, 2-aminoisobutyric acid (Aib), to stabilize the α-helix structure and to provide resistance to peptidases.

1. Introduction

Emergence of HIV-1 variants resistant to clinically approved inhibitors such as reverse transcriptase (RT) or viral protease is a serious problem in AIDS treatment.[1] Therefore, development of novel anti-HIV-1 drugs suppressing such resistant variants is urgently required. In this regard, inhibitors that target other processes, including integration, receptor binding or fusion have been proposed to suppress such resistant variants.[2–6] We and others have recently focused on viral fusion to host cells for development of novel anti-HIV agents that effectively inhibit HIV-1 replication with fewer resistant variants and adverse side effects.[7–9] Among envelope glycoproteins, gp41 in particular plays a pivotal role in the fusion process. Briefly, gp41 in trimer anchors to the host cell membrane, and two extra-virion α-helical regions, designated as heptad repeats 1 and 2 (HR1 and HR2), form an anti-parallel 6-helix bundle by the interaction between HR1 and HR2, leading to fusion of HIV-1 with the cell membrane.[10]

Enfuvirtide (T-20) **1**, which is derived from the gp41 HR2 region, is the only clinically approved peptide fusion inhibitor.[11] Although this agent is effective against variants resistant to multiple RT- and protease-inhibitors as well as wild-type strains,[12,13] T-20-resistant HIV-1 strains have emerged after T-20-containing therapy.[14,15] Thus, the development of second generation fusion inhibitors that suppress T-20-resistant variants is urgently needed. T-20 **1** and another HR2 peptide C34 **2** show the anti-HIV activity by binding with the viral gp41 HR1 to disturb the 6-helix bundle formation (Table 1).[10a] Previously, we developed the novel potent fusion inhibitors T-20EK[16] **3** and SC35EK[9] **4**, which are derived from T-20 **1** and C34 **2**, respectively. On the basis of the α-helical structure of these HR2 peptides upon binding with HR1,[17] we distinguished two surfaces: a virus HR1 interactive site and a solvent-accessible site (Fig. 1). For the residues at the solvent-accessible site (b, c, f, and g in Fig. 1), a series of systematic replacements with hydrophilic glutamic acid (E) or lysine (K) was introduced (EK motif) to enhance the α-helicity of the HR2 peptides by possible intrahelical salt-bridges. On the other hand, the residues at the interactive site (a, d, and e in Fig. 1) were retained for binding affinity. The stabilized bioactive α-helix conformation led to increased anti-HIV-1 activity through higher affinity with the virus HR1 region. 2-Aminoisobutyric acid (Aib), which could enhance and/or stabilize α-helicity of the peptides,[18,19] and may confer peptidase resistance,[20] was also applied to the modification of α-helix inducible EK motifs.

In this study, we investigated the minimal sequence of C34 **2** and SC35EK **4** for potent anti-HIV activity. In addition, modifications of each EK motif with Aib-containing motifs were examined.

2. Results and discussion

We and other groups have reported that C34 **2** and its derivatives interact with N36, a representative peptide of the gp41 HR1

* Corresponding author. Tel.: +81 75 753 4551; fax: +81 75 753 4570.
E-mail address: nfujii@pharm.kyoto-u.ac.jp (N. Fujii).

0968-0896/$ - see front matter © 2008 Elsevier Ltd. All rights reserved.
doi:10.1016/j.bmc.2008.09.018

Table 1
Sequences and anti-HIV activities of C34 and its derivatives, and T_m values of the mixture with N36

Peptide		Sequence	EC_{50} (nM)[a]	T_m (°C)[b]
T-20	1	YTSLIHSLIEESQNQQEKNEQELLELDKWASLWNWF	15	ND[c]
C34	2	WMEWDREINNYTSLIHSLIEESQNQQEKNEQELL	0.68	52.5
T-20EK	3	YTSLIEELIKKSEEQQKKNEEELKKLEEWAKKWNWF	1.8	N.D.[c]
SC35EK	4	WEEWDKKIEEYTKKIEELIKKSEEQQKKNEEELKK	0.39	71.5
C29	5	WMEWDREINNYTSLIHSLIEESQNQQEKN	46	48.5
C22	6	WMEWDREINNYTSLIHSLIERS	>1000	38.5
SC29EK	7	WEEWDKKIEEYTKKIEELIKKSEEQQKKN	0.46	65.0
SC22EK	8	WEEWDKKIEEYTKKIEELIKKS	60	63.5

[a] EC_{50} was determined as the concentration that blocked HIV-1 replication by 50%.
[b] T_m values were defined by the midpoint of the thermal unfolding transition state (Fig. 4).
[c] ND, not determined.

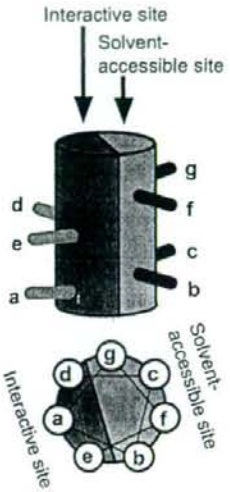

Figure 1. The design concept and helical wheel representation of HIV-1 gp41 HR2 peptide analogues. In the heptad repeat of α-helix, positions a, d, e and positions b, c, f, g represent the viral HR1 interactive and solvent-accessible site, respectively.

region.[9,19,21] In these reports, N-terminal tryptophan rich domain (WRD) containing two tryptophan residues of C34 **2** is essential for the interaction with the HR1 region,[22] while the C-terminal sequence might not be important compared to the N-terminal.[19,23] In order to identify the minimal N-terminal sequence of C34 **2** and SC35EK **4**, we designed two C-terminally truncated peptides C29 **5** and C22 **6** as well as the EK-motif-containing congeners SC29EK **7** and SC22EK **8**, respectively (Table 1). The anti-HIV activity of these peptides was examined by MAGI assay.[24,25] C29 **5** and C22 **6** showed marginal activity compared to the original C34 **2**,[19,26,27] while anti-HIV activity of SC29EK **7** possessing four EK motifs was comparable to that of C34 **2** and SC35EK **4**. Further truncation of an EK motif resulted in a significant decrease in anti-HIV activity (SC22EK **8**; EC_{50} = 60 nM). It is of note that SC29EK **7** and SC22EK **8** with EK motifs showed more potent activity than the original peptides C29 **5** and C22 **6**, respectively.

The potent anti-HIV activity of HR2-derived fusion inhibitors can be rationalized by the facilitated bioactive α-helix conformation, which is favorable for binding with the gp41 HR1 region.[9,28] Wavelength-dependent circular dichroism (CD) spectra of SC29EK **7** at 25 °C showed characteristic spectrum minima at 208 and 222 nm, which indicate the presence of a stable α-helical conformation, as observed in SC35EK **4** (Fig. 2). On the other hand, SC22EK **8** showed slightly less α-helicity compared with SC35EK **4** and SC29EK **7**, indicating that the truncated sequence of **8** may be insufficient to stabilize the α-helix structure. Native peptides, C34 **2**, C29 **5**, and C22 **6** exhibited similar spectra indicating the random structure (Fig. 2).

The binding affinities were estimated by measuring the CD spectra of HR2 peptides **2** and **4–8** in the presence of equimolar amount of N36 (HR1 region peptide). Similar spectra were observed in all N36/C34 derivative complexes except for the N36/C22 **6** complex, indicating that these peptide mixtures contained the similar stable 6-helix conformation at 25 °C (Fig. 3). Less stable coiled-coil structure of the N36/C22 **6** complex was consistent with the deficient anti-HIV activity of C22 **6**. Thermal stabilities of possible 6-helix bundle structures consisting of N36 and C34 derivatives were also evaluated by monitoring the CD signal at 222 nm. Melting temperature (T_m) of the complex was defined as the midpoint of thermal unfolding transition state shown in CD profiles (Fig. 4). T_m values of N36/SC35EK **4**, N36/SC29EK **7**, and N36/SC22EK **8** mixtures were 71.5, 65.0, and 63.5 °C, respectively, which were higher than those of the corresponding mixtures of native sequences [T_m (N36/C34 **2**) = 52.5 °C, T_m (N36/C29 **5**) = 48.5 °C, and T_m (N36/C22 **6**) = 38.5 °C] (Fig. 4). These results indicate that the introduction of EK motifs to HR2 peptides enhances binding affinity with the HR1 region, which could provide more potent anti-HIV activity. It should be noted that SC22EK **8** showed less potent anti-HIV activity compared with the other EK motif-containing peptides, although the thermal stabilities were similar. The limited coverage of the HR1 region by the truncated sequence of **8** may be inadequate for complete inhibition against folding of viral gp41 even with high binding affinity. As such, the potent anti-HIV activity of SC29EK **7** is rationalized by the presence of minimal interactive residues as well as the stabilized bioactive α-helix conformation induced by EK motifs.

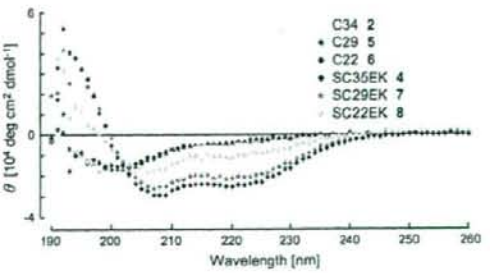

Figure 2. CD spectra of HR2 peptide analogues.

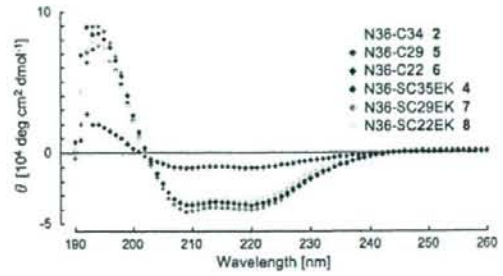

Figure 3. CD spectra of HR2 peptide analogues in the presence of equimolar amount of N36.

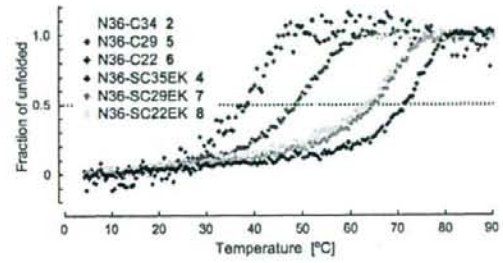

Figure 4. Thermal midpoint analysis of CD signal at 222 nm for HR1 (N36) and HR2 peptide complex.

Since the residues at the solvent-accessible sites of HR2 peptides have no direct involvement in the interaction with the viral HR1 region, we expected that these EK motifs could be replaced with other α-helix-inducible units. Replacement of a part of the EK motifs in SC29EK **7** with a pair of Aib-containing dipeptides such as Aib-Glu (***aE***) and Aib-Lys (***aK***) was attempted (peptides **9–12**, Fig. 5 and Table 2).[18,20] Anti-HIV activities of the Aib-substituted peptides **9–12** were equipotent or lower compared with SC29EK **7**. Peptide **9**, which was modified with a pair of ***aE*** and ***aK*** dipeptides at the essential WRD of the HR2 peptide[22] was the most potent, with the bioactivity almost identical to that of the parent SC29EK **7** (Table 2). This indicated that EK residues could be replaced with non-proteinogenic and α-helix inducible Aib residues, which may also enhance the biostability in vivo. In order to investigate the effect of the remaining Glu-Lys pairing in the ***aE/aK*** motif, we further substituted these residues with glycine (Gly)

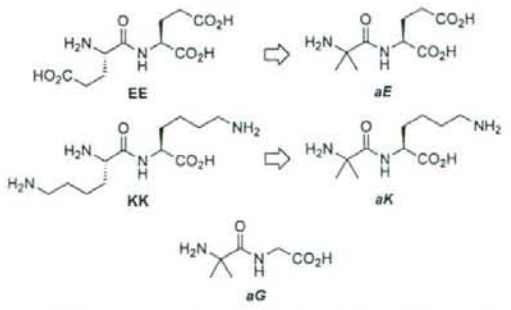

Figure 5. Substitution of an EE or KK unit with Aib-Glu (***aE***), Aib-Lys (***aK***), or Aib-Gly (***aG***).

Table 2
Sequences and anti-HIV activities of SC29EK analogues containing aminoisobutyric acid (Aib) residue

Peptide	Sequence	EC_{50}[a] (nM)
7	WEEWDKKIEEYTKKIEELIKKSEEQQKKN	0.46
9	W*a*EWD*a*KIEEYTKKIEELIKKSEEQQKKN	0.54
10	WEEWDKKI*a*EYT*a*KIEELIKKSEEQQKKN	2.15
11	WEEWDKKIEEYTKKI*a*ELI*a*KSEEQQKKN	0.87
12	WEEWDKKIEEYTKKIEELIKKS*a*E*a*KQQ*a*KN	7.10
13	W*a*GWD*a*GIEEYTKKIEELIKKSEEQQKKN	37.5
14	WEEWDKKI*a*GYT*a*GIEELIKKSEEQQKKN	270
15	WEEWDKKIEEYTKKI*a*GLI*a*GSEEQQKKN	25.6
16	WEEWDKKIEEYTKKIEELIKKS*a*GQQ*a*GN	31.3

[a] EC_{50} was determined as the concentration that blocked HIV-1 replication by 50%.

(peptides **13–16**) (Fig. 5 and Table 2). All substituted peptides **13–16** showed significantly less potent anti-HIV activity compared with the corresponding peptides **9–12** containing an ***aE/aK*** motif (Table 2), suggesting that modification of an EK motif with two Aib-Gly (***aG***) is not suitable for potent anti-HIV activity.

3. Conclusions

In this study, we identified the minimal bioactive sequence of HIV-1 fusion inhibitors and developed a novel potent fusion inhibitory peptide SC29EK **7** based on the previously reported SC35EK **4**. SC29EK **7** reproduced potent anti-HIV-1 activity comparable to SC35EK **4**. The introduction of α-helix-inducible EK motifs to less potent C29 **5** recovered the bioactivity of the parent C34 **2**, indicating that binding of the C29 sequence containing essential tryptophan rich domain to the gp41 HR1 is sufficient for anti-HIV activity. Moreover, it was also demonstrated that some EK motifs are replaceable with other non-proteinogenic amino acids such as 2-aminoisobutyric acid (Aib). These results may lead to development of more potent HIV-1 fusion inhibitors.

4. Experimental

4.1. Peptide synthesis

Protected peptide-resins were manually constructed by Fmoc-based solid-phase peptide synthesis. *t*-Bu ester for Asp and Glu; 2,2,4,6,7-pentamethyldihydrobenzofuran-5-sulfonyl (Pbf) for Arg; *t*-Bu for Thr; Tyr and Ser; Boc for Lys; and Trt for Gln, Asn, and His were employed for side-chain protection. Fmoc-amino acids were coupled using five equivalents of reagents [Fmoc-amino acid, *N*,*N*′-diisopropylcarbodiimide (DIPCDI), and HOBt·H_2O] in DMF for 1.5 h. Fmoc deprotection was performed with 20% piperidine in DMF (2 × 1 min, 1 × 20 min). The resulting protected resin was treated with TFA/thioanisole/*m*-cresol/1,2-ethandithiol/H_2O (80:5:5:5:5) at room temperature for 2 h. After removal of the resin by filtration, the filtrate was poured into ice-cold dry diethyl ether. The resulting powder was collected by centrifugation and washed with ice-cold dry diethyl ether. The crude product was purified by preparative HPLC on a Cosmosil 5C18-ARII preparative column (Nacalai Tesque, 20 × 250 mm, flow rate 10 mL/min) to afford the expected peptides. All peptides were characterized by an ESI-MS (Sciex API*III*E, Toronto, Canada) or MALDI-TOF-MS (AXIMA-CFR plus, Shimadzu, Kyoto, Japan), and the purity was calculated as >95% by HPLC on a Cosmosil 5C18-ARII analytical column (Nacalai Tesque, 4.6 × 250 mm, flow rate 1 mL/min) at 220 nm absorbance. The detailed MS data are shown in Table 3.

Table 3
Mass spectrum data of synthesized peptides

Peptide	Calculated MW ($M+H^+$)		Observed MW
1	$C_{204}H_{302}N_{51}O_{64}$	4492.9	4492.5[a]
2	$C_{186}H_{284}N_{51}O_{64}S$	4290.6	4289.3[a]
3	$C_{213}H_{329}N_{52}O_{63}$	4626.2	4625.5[a]
4	$C_{203}H_{326}N_{51}O_{66}$	4537.1	4536.3[a]
5	$C_{159}H_{240}N_{45}O_{54}S$	3677.9	3677.7[a]
6	$C_{125}H_{185}N_{32}O_{40}S$	2808.1	2808.1[a]
7	$C_{170}H_{270}N_{43}O_{54}$	3780.2	3779.5[a]
8	$C_{134}H_{210}N_{31}O_{40}$	2895.3	2895.2[a]
9	$C_{167}H_{265}N_{42}O_{52}$	3693.1	3693.5[b]
10	$C_{167}H_{265}N_{42}O_{52}$	3693.1	3693.5[b]
11	$C_{167}H_{265}N_{42}O_{52}$	3693.1	3692.5[b]
12	$C_{167}H_{265}N_{42}O_{52}$	3693.1	3693.8[b]
13	$C_{160}H_{252}N_{41}O_{50}$	3550.0	3550.1[b]
14	$C_{160}H_{252}N_{41}O_{50}$	3550.0	3549.5[b]
15	$C_{160}H_{252}N_{41}O_{50}$	3550.0	3550.2[b]
16	$C_{160}H_{252}N_{41}O_{50}$	3550.0	3550.2[b]

[a] MALDI-TOF-MS.
[b] ESI-MS (reconstructed).

4.2. Viruses and cells

An infectious clone pNL4-3 (GenBank Accession No. AF324493) was used for the construction and production of HIV-1 as described previously.[29] A wild-type HIV-1 was generated by transfection of pNL4-3 into 293T cells. HeLa-CD4-LTR-β-gal cells (MAGI cells) were kindly provided by Dr. Emerman through the AIDS Research and Reference Reagent Program, Division of AIDS, National Institute of Allergy and Infectious Disease (NIAID) (Bethesda, MD, USA).

4.3. Anti-HIV-1 activity

Anti-HIV-1 activity was determined by the multinuclear activation of a galactosidase indicator (MAGI) assay as described previously.[24,25] Briefly, the MAGI cells (10^4 cells/well) were seeded in flat bottomed 96-well microtitre plates. The following day, the cells were inoculated with HIV-1 (60 MAGI units/well, yielding 60 blue cells after 48 h incubation) and cultured in the presence of various concentrations of peptide inhibitors in fresh medium. After 48 h incubation, all the blue cells stained with 5-bromo-4-chloro-3-indolyl-β-D-galactopyranoside (X-gal) in each well were counted. The activity of inhibitors was determined as the concentration that blocked HIV-1 replication by 50% (50% effective concentration [EC_{50}]).

4.4. CD measurement

An HR2 peptide (peptides **2** and **4–8**) was dissolved in PBS pH 7.4 at a concentration of 10 μM. At the CD measurement of mixture of an HR1 peptide (N36) and an HR2 peptide or its analogues, the peptides were incubated at 37 °C for 30 min (final concentration of both HR1 peptide and HR2 peptide was 10 μM in PBS, pH 7.4). The wavelength-dependent of molar ellipticity [θ] was monitored at 25 °C as the average of eight scans, and the thermal stability of the HR1 and HR2 mixture was estimated by monitoring the change in the CD signal at 222 nm in a spectropolarimeter (Model J-710; Jasco, Tokyo, Japan) equipped with a thermoelectric temperature controller. The midpoint of thermal unfolding transition (melting temperature [T_m]) of each complex was determined as described previously.[9]

Acknowledgments

This work was supported in part by grants for the Promotion of AIDS Research from the Ministry of Health and Welfare and the Ministry of Education, Culture, Sports, Science, and Technology of Japan (E.K. and S.O.); a grant for Research for Health Sciences Focusing on Drug Innovation from The Japan Health Sciences Foundation (E.K., S.O., N.F., and M.M.); and the 21st Century COE program "Knowledge Information Infrastructure for Genome Science" (N.F. and H.N.). H.N. is grateful for the JSPS Research Fellowships for Young Scientists. Appreciation is expressed to Mr. Maxwell Reback (Kyoto University) for reading the manuscript.

References and notes

1. Clavel, F.; Hance, A. J. *N. Engl. J. Med.* **2004**, *350*, 1023.
2. Fatkenheuer, G.; Pozniak, A. L.; Johnson, M. A.; Plettenberg, A.; Staszewski, S.; Hoepelman, A. I.; Saag, M. S.; Goebel, F. D.; Rockstroh, J. K.; Dezube, B. J.; Jenkins, T. M.; Medhurst, C.; Sullivan, J. F.; Ridgway, C.; Abel, S.; James, I. T.; Youle, M.; van der Ryst, E. *Nat. Med.* **2005**, *11*, 1170.
3. Grinsztejn, B.; Nguyen, B. Y.; Katlama, C.; Gatell, J. M.; Lazzarin, A.; Vittecoq, D.; Gonzalez, C. J.; Chen, J.; Harvey, C. M.; Isaacs, R. D. *Lancet* **2007**, *369*, 1261.
4. Hazuda, D. J.; Young, S. D.; Guare, J. P.; Anthony, N. J.; Gomez, R. P.; Wai, J. S.; Vacca, J. P.; Handt, L.; Motzel, S. L.; Klein, H. J.; Dornadula, G.; Danovich, R. M.; Witmer, M. V.; Wilson, K. A.; Tussey, L.; Schleif, W. A.; Gabryelski, L. S.; Jin, L.; Miller, M. D.; Casimiro, D. R.; Emini, E. A.; Shiver, J. W. *Science* **2004**, *305*, 528.
5. Root, M. J.; Kay, M. S.; Kim, P. S. *Science* **2001**, *291*, 884.
6. Tagat, J. R.; McCombie, S. W.; Nazareno, D.; Labroli, M. A.; Xiao, Y.; Steensma, R. W.; Strizki, J. M.; Baroudy, B. M.; Cox, K.; Lachowicz, J.; Varty, G.; Watkins, R. J. *Med. Chem.* **2004**, *47*, 2405.
7. Bewley, C. A.; Louis, J. M.; Ghirlando, R.; Clore, G. M. *J. Biol. Chem.* **2002**, *277*, 14238.
8. Dwyer, J. J.; Wilson, K. L.; Davison, D. K.; Freel, S. A.; Seedorff, J. E.; Wring, S. A.; Tvermoes, N. A.; Matthews, T. J.; Greenberg, M. L.; Delmedico, M. K. *Proc. Natl. Acad. Sci. U.S.A.* **2007**, *104*, 12772.
9. Otaka, A.; Nakamura, M.; Nameki, D.; Kodama, E.; Uchiyama, S.; Nakamura, S.; Nakano, H.; Tamamura, H.; Kobayashi, Y.; Matsuoka, M.; Fujii, N. *Angew. Chem. Int. Ed. Engl.* **2002**, *41*, 2937.
10. (a) Chan, D. C.; Kim, P. S. *Cell* **1998**, *93*, 681; (b) Eckert, D. M.; Kim, P. S. *Annu. Rev. Biochem.* **2001**, *70*, 777.
11. Matthews, T.; Salgo, M.; Greenberg, M.; Chung, J.; DeMasi, R.; Bolognesi, D. *Nat. Rev. Drug Discov.* **2004**, *3*, 215.
12. Lalezari, J. P.; Henry, K.; O'Hearn, M.; Montaner, J. S.; Piliero, P. J.; Trottier, B.; Walmsley, S.; Cohen, C.; Kuritzkes, D. R.; Eron, J. J., Jr.; Chung, J.; DeMasi, R.; Donatacci, L.; Drobnes, C.; Delehanty, J.; Salgo, M. *N. Engl. J. Med.* **2003**, *348*, 2175.
13. Lazzarin, A.; Clotet, B.; Cooper, D.; Reynes, J.; Arasteh, K.; Nelson, M.; Katlama, C.; Stellbrink, H. J.; Delfraissy, J. F.; Lange, J.; Huson, L.; DeMasi, R.; Wat, C.; Delehanty, J.; Drobnes, C.; Salgo, M. *N. Engl. J. Med.* **2003**, *348*, 2186.
14. Poveda, E.; Rodes, B.; Toro, C.; Martin-Carbonero, L.; Gonzalez-Lahoz, J.; Soriano, V. *AIDS* **2002**, *16*, 1959.
15. Wei, X.; Decker, J. M.; Liu, H.; Zhang, Z.; Arani, R. B.; Kilby, J. M.; Saag, M. S.; Wu, X.; Shaw, G. M.; Kappes, J. C. *Antimicrob. Agents Chemother.* **2002**, *46*, 1896.
16. Oishi, S.; Ito, S.; Nishikawa, H.; Watanabe, K.; Tanaka, M.; Ohno, H.; Izumi, K.; Sakagami, Y.; Kodama, E.; Matsuoka, M.; Fujii, N. *J. Med. Chem.* **2008**, *51*, 388.
17. Chan, D. C.; Fass, D.; Berger, J. M.; Kim, P. S. *Cell* **1997**, *89*, 263.
18. Karle, I. L.; Balaram, P. *Biochemistry* **1990**, *29*, 6747.
19. Sia, S. K.; Carr, P. A.; Cochran, A. G.; Malashkevich, V. N.; Kim, P. S. *Proc. Natl. Acad. Sci. U.S.A.* **2002**, *99*, 14664.
20. Yamaguchi, H.; Kodama, H.; Osada, S.; Kato, F.; Jelokhani-Niaraki, M.; Kondo, M. *Biosci. Biotechnol. Biochem.* **2003**, *67*, 2269.
21. Liu, S.; Lu, H.; Niu, J.; Xu, Y.; Wu, S.; Jiang, S. *J. Biol. Chem.* **2005**, *280*, 11259.
22. Chan, D. C.; Chutkowski, C. T.; Kim, P. S. *Proc. Natl. Acad. Sci. U.S.A.* **1998**, *95*, 15613.
23. Gochin, M.; Savage, R.; Hinckley, S.; Cai, L. *Biol. Chem.* **2006**, *387*, 477.
24. Kimpton, J.; Emerman, M. *J. Virol.* **1992**, *66*, 2232.
25. Kodama, E. I.; Kohgo, S.; Kitano, K.; Machida, H.; Gatanaga, H.; Shigeta, S.; Matsuoka, M.; Ohrui, H.; Mitsuya, H. *Antimicrob. Agents Chemother.* **2001**, *45*, 1539.
26. Ji, H.; Shu, W.; Burling, F. T.; Jiang, S.; Lu, M. *J. Virol.* **1999**, *73*, 8578.
27. Shu, W.; Liu, J.; Ji, H.; Radigen, L.; Jiang, S.; Lu, M. *Biochemistry* **2000**, *39*, 1634.
28. Judice, J. K.; Tom, J. Y.; Huang, W.; Wrin, T.; Vennari, J.; Petropoulos, C. J.; McDowell, R. S. *Proc. Natl. Acad. Sci. U.S.A.* **1997**, *94*, 13426.
29. Nameki, D.; Kodama, E.; Ikeuchi, M.; Mabuchi, N.; Otaka, A.; Tamamura, H.; Ohno, M.; Fujii, N.; Matsuoka, M. *J. Virol.* **2005**, *79*, 764.

Original article

Binding modes of two novel non-nucleoside reverse transcriptase inhibitors, YM-215389 and YM-228855, to HIV type-1 reverse transcriptase

Eiichi Kodama[1], Masaya Orita[2], Naoyuki Masuda[2], Osamu Yamamoto[2], Masahiro Fujii[2], Tetsuro Ohgami[2], Shunji Kageyama[2], Mitsuaki Ohta[2], Toshifumi Hatta[2], Hiroshi Inoue[2], Hiroshi Suzuki[2], Kenji Sudo[2], Yasuaki Shimizu[2] and Masao Matsuoka[1]*

[1]Laboratory of Virus Control, Institute for Virus Research, Kyoto University, Kyoto, Japan
[2]Drug Discovery Research, Astellas Pharma Inc., Tsukuba, Japan

*Corresponding author: E-mail: ekodama@virus.kyoto-u.ac.jp

Background: YM-215389 and YM-228855 are thiazolidenebenzenesulfonamide (TBS) derivatives and novel non-nucleoside reverse transcriptase inhibitors (NNRTIs) that inhibit not only wild-type, but also the K103N- and Y181C-substituted reverse transcriptase (RT) of HIV type-1 (HIV-1).

Methods: To characterize the binding modes of the TBS derivatives in detail, the anti-HIV-1 activities of YM-215389 and YM-228855 against various NNRTI-resistant clones were examined. Docking studies with HIV-1 RT were also performed.

Results: YM-215389, which effectively inhibits various NNRTI-resistant clones, interacted with L100, K103, V106 and Y318 through the benzene ring and with E138, V179, Y181, Y188 and W229 through the thiazole ring. A single amino acid substitution confers only moderate resistance to YM-215389; indeed, four amino acid substitutions (V106L, V108I, E138K and L214F) were necessary for high-level resistance. Although the activity of YM-228855, a derivative of YM-215389 that has two bulky and rigid cyano-moieties on the benzene ring, was 10× more potent against HIV-1 than YM-215389, its anti-HIV-1 activity was readily reduced with single substitutions as with Y181I and K103N.

Conclusions: These results provide structural information for optimizing the TBS derivatives in an attempt to construct ideal NNRTIs that maintain anti-HIV-1 activity to various HIV-1 variants.

Introduction

Allosteric inhibitors bind to a specific site on a target protein that differs from the substrate binding site and alters the conformation of the protein, resulting in a loss of protein function. Allosteric inhibitors for HIV type-1 (HIV-1) reverse transcriptase (RT), designated as non-nucleoside RT inhibitors (NNRTIs), are widely used for HIV-1-infected patients. NNRTIs bind to the NNRTI-binding hydrophobic pockets (NNRTI-BHP) located close to the RT active site and cause a conformational distortion to inactivate the enzyme [1].

Of the clinically approved NNRTIs, nevirapine (NVP) is used for pregnant women infected with HIV-1 to reduce the incidence of peripartum infection without severe adverse effects [2]. NVP combined with zidovudine (3′-azido-3′-deoxythymidine [AZT]) also effectively suppresses mother-to-child transmission during labour [3]. Efavirenz (EFV), another approved NNRTI, potently inhibits HIV-1 replication *in vitro* and in clinical cases [4]. In a clinical study, EFV administered with two nucleos(t)ide RT inhibitors (NRTIs) is more effective than a protease inhibitor administered with two NRTIs [5]. Moreover, during the initial treatment of HIV-1 infection, regimens that include EFV experience fewer treatment failures compared with regimens that include the NRTIs only [6–8]. Thus, the NNRTIs play an important role in the chemotherapy for HIV-1-infected patients.

Although NNRTIs potently inhibit HIV-1 replication, HIV-1 rapidly acquires resistance to NNRTIs, both *in vitro* and *in vivo*, through a conformational change in the NNRTI-BHP that is caused by mutations. NVP loses its anti-HIV-1 activity against HIV-1 variants that have amino acid substitutions, for example, lysine to aspartic acid at amino acid position 103 in the RT (K103N) or

Y181C variant [9–11]. The K103N variant and NNRTI-related double mutation, for example, K103N plus Y188L, carry high resistance to EFV [12,13]. Therefore, the development of NNRTIs, which maintain anti-HIV-1 activity against various NNRTI-resistant variants, is important to sustain long-term HIV-1 chemotherapy.

We recently reported that novel NNRTIs, the thiazolidenebenzenesulfonamide (TBS) derivatives YM-215389 and YM-228855 (Figure 1A), inhibited HIV-1 replication, including that of the K103N- and Y181C-substituted variants [14–16]. To elucidate YM-215389 and YM-228855 binding to HIV-1 RT, the anti-HIV-1 activity of these two TBS derivatives against NNRTI-resistant clones was measured. In addition, genotypic and phenotypic analyses of variants resistant to YM-215389 and YM-228855, as well as docking studies on these TBS derivatives with HIV-1 RT were performed. Our data provide useful structural information to optimize TBS derivatives for the ideal NNRTIs that maintain anti-HIV-1 activity to various HIV-1 variants.

Methods

Antiviral agents

AZT was purchased from Sigma (St Louis, MO, USA). NNRTIs, NVP, EFV, YM-215389 and YM-228855 were synthesized as described previously [14,17].

Cells

MT-2 and 293T cells were grown in RPMI 1640 medium and Dulbecco's modified Eagle's medium, respectively, supplemented with 10% fetal calf serum, 2 mM L-glutamine, 100 U/ml penicillin and 50 μg/ml streptomycin. HeLa-CD4-LTR/β-gal cells [18] were used to determine drug susceptibility.

Viruses and construction of HIV-1 clones

The laboratory strain, HIV-1_{LAI}, propagated in MT-2 cells, was employed for induction of the resistant variants. Recombinant infectious HIV-1 clones carrying various substitutions in the RT gene were generated as described previously [19]. Briefly, desired mutations were introduced into the *Xma*I–*Nhe*I region (759 base pairs) of pTZNX1, which codes for Gly-15 to Ala-267 of HIV-1 RT (strain BH10), by site-directed mutagenesis. The *Xma*I–*Nhe*I fragment was inserted into a pNL101-based plasmid, pNL–RT, generating various molecular clones with the desired mutations. The presence of the intended substitutions and the absence of unintended substitutions in the infectious clones were confirmed by sequencing.

Each molecular clone was transfected into 293T cells and cocultured with MT-2 cells after 24 h. When an extensive cytopathic effect was observed, cell-free supernatants were harvested, titrated for virus and stored at -80°C until use. An infectious clone generated from pNL–RT served as a wild-type infectious clone (HIV-1_{WT}).

Determination of drug susceptibility

The sensitivity of infectious clones to various RT inhibitors was determined using the multinuclear activation of a galactosidase indicator (MAGI) assay [18] with some modifications [19,20]. Briefly, HeLa CD4-LTR/β-gal cells (10^4 cells/well) were plated in 96-well flat microtitre culture plates. On the following day, the medium was aspirated and the cells were inoculated with the HIV-1 clones (70 MAGI units/well, which yielded 70 blue cells after 48 h of incubation) and cultured in the presence of various concentrations of drugs in fresh medium. The blue cells in each well were counted 48 h after viral exposure. All experiments were performed in triplicate.

Induction of resistant variants

MT-2 cells and HIV-1_{LAI} were used for induction of resistant variants using a dose-escalating method [20,21]. Each selection experiment began at the 50% effective concentration (EC_{50}) determined by the MAGI assay. When extensive cytopathic effects were observed, the concentration was increased to twice the initial concentration. The sequence of the RT region was determined using direct sequencing of the proviral DNA from the infected MT-2 cells.

Molecular modelling and docking studies

Three dimensional structures of YM-215389 and YM-228855 were generated using the previously determined crystal structure of the parental compound, *N*-(5-tert-butyl-3,4-dimethyl-1,3-thiazol-2(3*H*)-ylidene)-3-nitrobenzenesulfonamide [14,17] as the template. Docking studies of the compounds and HIV-1 RT were performed using the GOLD program [22] on the HIV-1 RT structure obtained from the Protein Data Bank (PDB) [23] for the 1HNV entry [24]. Structures of reference compounds, NVP and EFV (PDB code 1FK9 and 1VRT [25], respectively), were also obtained from the PDB. In these models, the amino acid substitution docking score for RT and the reference compounds were calculated using the SYBYL program, version 6.8 (Tripos, St Louis, MO, USA). To estimate the flexibility of YM-215389, we analysed the torsion angle distributions of the single rotation bond between the thiazole ring and the benzene ring using the Cambridge Structural Database (CSD) [26].

Results

Anti-HIV-1 activity of the TBS derivatives to NNRTI-resistant clones

The anti-HIV-1 activities of YM-215389 and YM-228855 against recombinant viruses with major NNRTI-resistant

substitutions (deposited in the Stanford HIV Drug Resistance Database [27,28]), were measured using the MAGI assay (Table 1). YM-215389 and YM-228855 inhibited six major substituted variants: HIV-1_{A98G}, HIV-1_{K103N}, HIV-1_{V106A}, HIV-1_{Y181C}, HIV-1_{V189I} and HIV-1_{G190A} with EC_{50} values at submicromolar concentrations. YM-215389 potently inhibited HIV-1_{V106A}, HIV-1_{Y181C} and HIV-1_{V189I} clones with EC_{50} values similar to that against HIV-1_{WT} (20 nM), but its anti-HIV-1 activity against HIV-1_{A98G}, HIV-1_{K103N} and HIV-1_{G190A} clones were somewhat less (7–33-fold resistance of HIV-1_{WT}). YM-228855, a derivative of YM-215389 that has two cyano-moieties on the phenyl ring, showed extremely potent anti-HIV-1 activity against HIV-1_{WT} (EC_{50}=2.0 nM). The anti-HIV-1 activity of YM-228855 against HIV-1_{A98G}, HIV-1_{K103N} and HIV-1_{Y181C} clones were less than against HIV-1_{WT} (17-, 87- and 54-fold, respectively). Interestingly, the anti-HIV-1 activity of YM-228855 against HIV-1_{V106A} and HIV-1_{V189I} was slightly more than against HIV-1_{WT}. Overall, the YM-215389 range of antiviral efficacy against NNRTI-resistant variants was larger than NVP and similar to EFV. However, the YM-228855 range of antiviral efficacy was similar to NVP, but worse than EFV and YM-215389 (Table 1).

Isolation and genotypic analyses of variants resistant to TBS derivatives

During serial passage (P) in the presence of YM-215389, at concentrations of <0.1 μM, a partial substitution of isoleucine for valine (V106V/I) and L214F substitutions were found at P-11 (Figure 1B). At P-16, V106V/I changed to solely V106I and additional partial substitutions, V108V/I and E138E/K, were identified. At P-20, at a concentration of >20 μM, the substitution of V106I changed to V106L and the partial substitutions V108V/I and E138E/K were completely changed to V108I and E138K, which resulted in a V106L, V108I, E138K and L214F combined mutant, HIV-$1_{YM\text{-}215389}{}^{R}$.

In the presence of YM-228855, at concentrations of <0.1 μM, T165I and L214F substitutions were found at P-16 (Figure 1C). These substitutions have not been reported as NNRTI-resistant substitutions, but are described as polymorphisms in the HIV-1 genome [29,30]. At P-24, partial substitutions for wild-type amino acids, V179V/D and Y188Y/C, were found in addition to the T165I and L214F mutations. However, at P-28, V179D disappeared and Y181Y/I emerged. At P-31, at concentrations >50 μM, T165I and Y188Y/C disappeared and the only detectable substitutions were

Table 1. Anti-HIV-1 activity of NNRTIs against various substituted variants

Virus	EC_{50}, nM (fold of resistance)				
	Zidovudine	Nevirapine	Efavirenz	YM-215389	YM-228855
HIV-$1_{NL\text{-}WT}$	32	40	0.5	20	2
Major NNRTI-resistant substitutions					
HIV-1_{A98G}	43 (1.3)*	192 (4.5)	2.7 (5.4)	184 (9.2)	34 (17)†
HIV-1_{K103N}	35 (1.1)	2,212 (55)†	47 (94)†	665 (33)†	199 (87)†
HIV-1_{V106A}	36 (1.1)	2,723 (68)†	2 (4)	22 (1.1)	0.4 (0.2)
HIV-1_{Y181C}	35 (1.1)	6,470 (160)†	0.7 (1.4)	46 (2.3)	107 (54)†
HIV-1_{V189I}	19 (0.6)	30 (0.8)	0.4 (0.8)	46 (2.3)	0.8 (0.4)
HIV-1_{G190A}	30 (1)	2,600 (65)†	4.5 (9)	145 (7.3)	12 (6)
Substitutions observed during selection with YM-215389					
HIV-1_{V106I}	18 (0.6)	94 (2)	0.7 (1.4)	52 (2.6)	3 (1.5)
HIV-1_{V106L}	21 (0.7)	33 (1)	0.5 (1)	310 (16)†	29 (15)†
HIV-1_{V108I}	1.9 (0.06)	473 (12)†	4.8 (10)†	66 (3.3)	4.8 (2.4)
HIV-1_{E138K}	2.8 (0.09)	156 (4)	2.5 (5)	174 (8.7)	10 (5)
HIV-1_{L214F}	6 (0.2)	69 (1.7)	1 (2)	35 (1.8)	3 (1.5)
HIV-$1_{V106I/E138K}$	10 (0.3)	430 (11)†	4 (8)	1,130 (57)†	43 (22)†
HIV-$1_{V106I/V108I/E138K}$	38 (1.2)	354 (9)	4 (8)	4,051 (200)†	44 (22)†
HIV-$1_{V106I/V108I/E138K}$	7 (0.2)	98 (2.5)	4 (8)	6,600 (330)†	106 (53)†
HIV-$1_{V106I/V108I/E138K/L214F}$	9 (0.3)	165 (4.1)	6 (12)†	>10,000 (>500)†	811 (400)†
Substitutions observed during selection with YM-228855					
HIV-1_{Y188C}	120 (4)	552 (14)	0.6 (1.2)	161 (8)	48 (24)
HIV-1_{Y181I}	30 (0.9)	7,150 (180)†	4.1 (8)	310 (16)†	1,084 (540)†
HIV-$1_{Y181I/L214F}$	25 (0.8)	>10,000 (>250)†	4 (8)	737 (37)†	2,874 (1,400)†

Data represent the mean values of at least three independent assays. The 50% antiviral effective concentration (EC_{50}) was determined from the multinuclear activation of a galactosidase indicator assay. *Fold of resistance compared with the HIV type-1 wild-type infectious clone (HIV-$1_{NL\text{-}WT}$). †Resistance >10-fold. NNRTI, non-nucleoside reverse transcriptase inhibitor.

Figure 1. Chemical structures of YM-215389 and YM-228855 and induction profiles of resistant variants

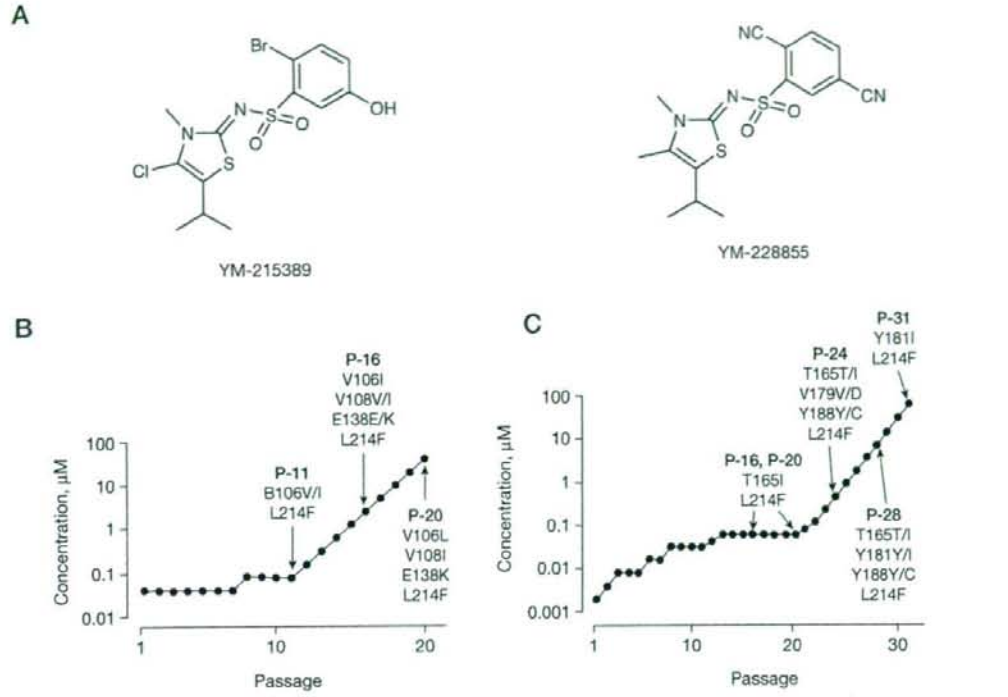

(A) Chemical structures of YM-215389 and YM-228855. The induction of resistant variants was performed using the dose-escalation method. (B) The HIV type-1 laboratory strain (HIV-1_{LAI}) was passed in the presence of increasing concentrations of YM-215389 and (C) YM-228855 in MT-2 cells. At the indicated passage (P), proviral DNA was extracted from HIV-1_{LAI}-infected MT-2 cells and subjected to PCR-mediated direct sequence analysis. The amino acid substitutions observed are shown. Each passage period was approximately 5–7 days.

Y181I and L214F (HIV-$1_{YM\text{-}228855}{}^{R}$). These changes might have some benefit for virus replication and/or the development of strong drug resistance. Although the resistant variants were selected in the presence of YM-215389 and YM-228855, which are structurally similar, their genotypes differ.

NNRTI-susceptibility of HIV-$1_{YM\text{-}215389}{}^{R}$ and HIV-$1_{YM\text{-}228855}{}^{R}$

YM-215389 and YM-228855 inhibited parental HIV-1_{LAI} replication (EC_{50} at 13 nM and 2.3 nM, respectively; Table 2). As expected, the variant resistant to YM-215389 (HIV-$1_{YM\text{-}215389}{}^{R}$) strongly reduced susceptibility to YM-215389 (>770-fold), but it showed only 140- and 17-fold reductions in susceptibility to YM-228855 and NVP, respectively. In contrast, the variant resistant to YM-228855 (HIV-$1_{YM\text{-}228855}{}^{R}$) exhibited high levels of resistance to YM-228855 (2,600-fold) and NVP (>250-fold), whereas it showed only 70-fold resistance to YM-215389. HIV-$1_{YM\text{-}215389}{}^{R}$ and HIV-$1_{YM\text{-}228855}{}^{R}$ showed a certain amount of cross-resistance to each other. Both variants showed a slight reduction in susceptibility to EFV (7–11-fold reduction). However, they showed different resistance phenotypes to NVP; HIV-$1_{YM\text{-}228855}{}^{R}$ reduced its susceptibility to NVP >15-fold stronger than HIV-$1_{YM\text{-}215389}{}^{R}$.

Effect of substitutions observed during the selection

To examine which substitution is involved in the development of YM-215389 and YM-228855 resistance, various molecular clones containing substitutions observed during the resistant variant selection were constructed. Among the substitutions obtained during HIV-$1_{YM\text{-}215389}{}^{R}$ selection, V106I, V106L and L214F substitutions did not confer any resistance to NVP or EFV (Table 1). The V106I substitution did not confer any resistance to TBS derivatives, whereas the V106L substitution resulted in modest resistance to YM-215389 and YM-228855 (16- and 15-fold reductions, respectively). The V108I substitution did not induce high resistance to TBS derivatives; however, it enhanced

Table 2. EC_{50} of NNRTIs for HIV-$1_{YM-215389}{}^{R}$ and HIV-$1_{YM-228855}{}^{R}$

Virus	EC_{50}, nM (fold of resistance)				
	Zidovudine	Nevirapine	Efavirenz	YM-215389	YM-228855
HIV-1_{IIIB}	21	40	0.7	13	2.3
HIV-$1_{YM-215389}{}^{R}$	6 (0.29)*	680 (17)	8 (11)	>10,000 (>770)	325 (140)
HIV-$1_{YM-228855}{}^{R}$	53 (2.5)	>10,000 (>250)	4.9 (7)	902 (69)	6,000 (2,600)

Data represent the mean values of at least three independent assays. The 50% antiviral effective concentration (EC_{50}) was determined from the multinuclear activation of a galactosidase indicator assay. *Fold of resistance compared with the HIV type-1 wild-type infectious clone (HIV-1_{NL-WT}). NNRTI, non-nucleoside reverse transcriptase inhibitor.

YM-215389 and YM-228855 resistance by E138K substitution. V108I and E138K substitutions are also observed during *in vitro* experiments with combination regimens containing EFV [31,32]. Comparisons of V106I/V108I/E138K with V106L/V108I/E138K also indicated that V106L enhanced drug resistance to TBS derivatives. This is consistent with observations made during selection; the V106I substitution was observed at P-16 (2.56 μM), but was replaced by V106L at P-20 (40 μM; Figure 1B). According to the Stanford HIV Drug Resistance Database, V106I is a common polymorphism that does not decrease NNRTI susceptibility. In contrast, V016L is rarely observed and only confers potential low-level resistance to NVP and delavirdine. Therefore, V106L appears to be a characteristic mutation for YM-215389.

The L214F substitution observed in many HIV-1 strains isolated from drug-naive patients [29] did not show resistance to any of the compounds tested. However, L214F enhanced resistance to YM-215389 when combined with V106L/V108I/E138K (Table 1). These results suggest that for the development of YM-215389 resistance, the primary mutation is V106L; however, other mutations are also needed to obtain stronger resistance (Table 1). L214F also played an important role in enhancing resistance to YM-228855 (Y181I with Y181I/L214F; Table 1).

Docking study

The modes in which YM-215389 and YM-228855 bind to HIV-1 RT were estimated using the GOLD program. Our simulation indicated that their binding modes are almost the same. As shown in Figures 2A–2D, 'the body' is formed by the hydrophilic sulfonamide faces outside of the NNRTI-BHP and 'the wings' are formed by the hydrophobic thiazole and benzene rings where they interact with the hydrophobic amino acids in the NNRTI-BHP, such as L100, K103, V106, Y318, E138, V179, Y181, Y188 and W229. YM-215389 interacts with L100, K103, V106 and Y318 through the benzene ring and with E138, V179, Y181, Y188 and W229 through the thiazole ring (Figure 2E). In our model, there was no hydrogen bonding between YM-215389 or YM-228855 and NNRTI-BHP. The T165 and L214 substitutions were located outside of the NNRTI-BHP and each had a slight effect on the binding of TBS derivatives to HIV-1 RT.

Structural comparison of TBS derivatives with NVP and EFV

The structures of YM-215389 and YM-228855 elucidated by our docking simulations were compared with those of NVP (1FK9) and EFV (1VRT). The TBS derivatives had a 'butterfly structure', like NVP and EFV (Figures 3A & 3B) [33,34]. The thiazole and benzene rings, and the sulfonamide region constitute the butterfly's left wing, right wing and body, respectively. Superimposition of the TBS derivatives' figures onto those of NVP and EFV shows that the wing and body sizes are similar to identical (Figure 3A). This indicates that TBS derivatives interact with the NNRTI-BHP in a manner similar to that of NVP and EFV.

Flexibility of TBS

In the CSD, 24 compounds with a thiazole ring-sulfonamide-benzene ring are deposited and were subjected to analysis of their torsion angles at C1-N2-S3-C4. The torsion angles were distributed between -123° to -64° and 71° to 129°. Conformational preferences for YM-215389 are depicted in Figure 4. Because the benzene ring must be in the upright position (as depicted in Figure 2) in order to interact with NNRTI-BHP, the torsion angle distribution of the wing-angle was estimated to be 71 to 129°, which suggests that the sulfonamide bond can be rotated intermediately.

Discussion

Currently available NNRTIs interact with the NNRTI-BHP close to the HIV-1 RT active site [35,36]. This common binding pocket results in cross-resistance among both first- and second-generation NNRTIs. For example, the K103N mutation located at the entrance to the NNRTI-BHP [37,38] reduces susceptibility to various NNRTIs. The transformation of the linearly charged amino acid lysine into uncharged and branched asparagine increases pocket volume and decreases interaction

Figure 2. Binding modes of YM-215389 and YM-228855 to NNRTI-BHP

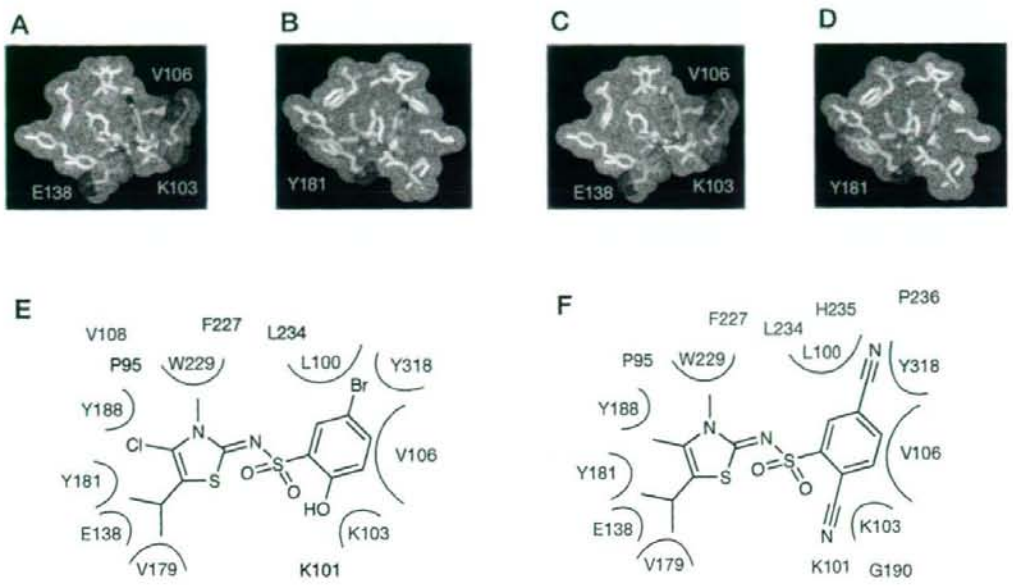

HIV type-1 (HIV-1) reverse transcriptase binding schemes (Protein Data Bank code 1HNV) [33] to (**A** & **B**) YM-215389 or (**C** & **D**) YM-228855 are shown. Blue, yellow and red indicate nitrogen, oxygen and sulfur, respectively. The K103 amino acid is indicated in orange and those of V106, E138 and Y181 are in green. Models of the interactions between the non-nucleoside reverse transcriptase inhibitor-binding hydrophobic pockets (NNRTI-BHP) and (**E**) YM-215389 and (**F**) YM-228855 are shown. The distances between YM-215389 and YM-228855 and the amino acids in the NNRTI-BHP are indicated in red (within 3.5 Å) and black (3.5–4.0 Å). V108 is indicated in blue (E) because the distance from the methyl moiety at the thiazole ring of YM-215389 is 6.8 Å.

with NNRTIs. It also stabilizes the unliganded closed conformation of the NNRTI-BHP [9,34].

For YM-215389, the effect of K103N mutation on its anti-HIV-1 activity was smaller than NVP, EFV and YM-228855 (Table 1). In fact, four amino acid substitutions were required for YM-215389 to develop strong resistance (>500-fold). Interestingly, all substituted mutants observed during HIV-$1_{YM\text{-}215389}{}^{R}$ selection increased the susceptibility to AZT. This means that the emergence of resistance to YM-215389 does not occur readily, especially when the drug is used in combination with AZT. These results suggest that YM-215389 is a valuable lead compound in the search for next generation NNRTIs. The docking study showed that YM-215389 interacts hydrophobically with multiple amino acids in NNRTI-BHP, that is, YM-215389 interacts uniformly with L100, K103, V106 and Y318 through the benzene ring, and with E138, V179, Y181, Y188 and W229 through the thiazole ring (Figures 2A, 2B & 2E). A single amino acid substitution over a large area within the NNRTI-BHP confers only moderate resistance to YM-215389 (Table 1). YM-215389 is thought to maintain its anti-HIV-1 activity to major NNRTI-resistant mutants by adjusting the hydrophobic interactions with NNRTI-BHP via a sulfonamide backbone that can be rotated intermediately. The anti-HIV-1 activity of YM-228855 (EC_{50}=2 nM) was more potent than that of YM-215389 (EC_{50}=20 nM). However, its potent anti-HIV-1 activity was strongly reduced by single amino acid substitutions (Y181I, K103N and Y181C substitutions resulted in 540-, 87- and 54-fold reductions, respectively). These results suggest that the cyano-moieties on the benzene ring of YM-228855 contribute to the enhanced anti-HIV-1 activity, but its protruding character restricts conformational adjustment with NNRTI-BHP.

The advantage of conformational adaptability has also been demonstrated with another NNRTI [39]. A diarylpyrimidine derivative, etravirine (TMC125-R165335) that inhibits various NNRTI-resistant clones with single amino acid substitutions, binds to the NNRTI-BHP using several binding modes. Cocrystallization of RT with etravirine results in resolution of only 6–8 Å (crystal grams), even when

using high-intensity synchrotron radiation, because the conformations corresponding with RT and etravirine that coexist in the crystal are different [40]. Like etravirine, YM-215389 has an intermediately rotatable sulfonamide backbone, which allows for more conformational adaptability than NVP and EFV can achieve. This is because NVP has a highly rigid dihydrodipyridodiazepine (triple ring) backbone and EFV has a relatively rigid 4-alkynyldihydrobenzoxazine-containing triple bond between its body and left wing.

It has also been reported that inhibitors carrying molecularly flexible groups tend to be able to adapt to mutated enzymes. For instance, tenofovir (9-*R*-2-phosphonomethoxypropyl adenine [PMPA]), an acyclic NRTI, inhibits various types of drug resistance to HIV-1 variants both *in vitro* and *in vivo* [41,42]. PMPA has a highly flexible acyclic sugar compared with other NRTIs, for example, 2′,3′-dideoxyinosine, which confers the advantages of NRTIs [43]. PMPA can bind even to a mutated 3′-OH binding site, for example, K65, R72, Y115 and Q151, and be incorporated into the elongating primer end to block it. The incorporated PMPA can also escape excision by ATP. Thus, PMPA effectively inhibits viral DNA synthesis mediated by RT with resistance mutations. It has also been reported that the flexible HIV-1 protease inhibitor, JE-2147, which contains a P2′ benzylamide group with two rotatable bonds, is able to inhibit various protease inhibitor-resistant variants. However, the inflexible derivative, JE-533, which contains a *t*-butylamide group with only one rotatable bond at this position, fails to suppress the resistant variants [44].

In this report, the anti-HIV-1 activities of YM-215389 and YM-228855 against various substituted variants were investigated. The data suggest that conformational adaptability of hydrophobic interactions is important for enabling NNRTIs to maintain their anti-HIV activity against various HIV-1 variants. Therefore, YM-215389 is considered to be a promising lead compound for the next generation of NNRTIs.

Acknowledgements

We would like to thank Miyuki Ino, Mieko Ikeuchi and Shuhei Taguwa for technical assistance and Ayako Yoshioka for the manuscript preparation. The HeLa-CD4-LTR/β-gal cells were kindly provided by Dr Michael Emerman through the AIDS Research and Reference Reagent Program, Division of AIDS, NIAID, NIH (Bethesda, MD, USA). The pNL101 plasmid was a kind gift from Dr Kuan-Teh Jeang (NIH). This work was supported in part by grants for the Promotion of AIDS Research from the Ministry of Health and Welfare and for the Ministry of Education, Culture, Sports, Science and Technology of Japan (EK), and a grant for Research for Health Sciences Focusing on Drug Innovation from The Japan Health Sciences Foundation (EK and MM).

Figure 3. Three-dimensional structures of YM-215389 and YM-228855

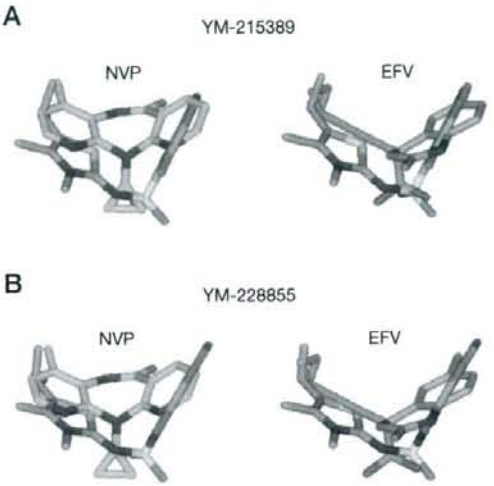

Superimposed comparisons of the three-dimensional structures of (A) YM-215389 to nevirapine (NVP) or efavirenz (EFV) and (B) YM-228855 to NVP or EFV are shown. Thiazole derivatives, NVP and EFV are indicated in gray, emerald and brown, respectively. Blue, yellow, red and green indicate nitrogen, sulfur, oxygen and fluorine, respectively.

Figure 4. Estimated flexibility of YM-215389

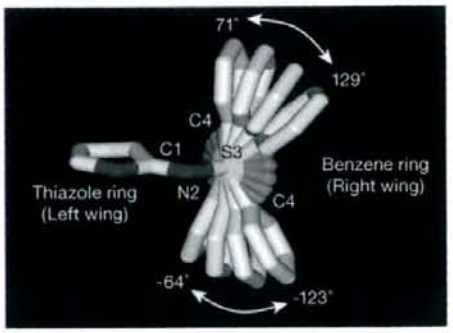

The flexibility of thiazolidenebenzenesulfonamide derivatives were estimated from 24 compounds with a thiazole ring-sulfonamide-benzene ring deposited in the Cambridge Structural Database [26]. The estimated torsion angles of C1-N2-S3-C4 are shown.

Disclosure statement

The authors declare no competing interests.

References

1. Tantillo C, Ding J, Jacobo-Molina A, *et al.* Locations of anti-AIDS drug binding sites and resistance mutations in the three-dimensional structure of HIV-1 reverse transcriptase. Implications for mechanisms of drug inhibition and resistance. *J Mol Biol* 1994; **243**:369–387.
2. Mitchla Z, Sharland M. Current treatment options to prevent perinatal transmission of HIV. *Expert Opin Pharmacother* 2000; **1**:239–248.
3. Lallemant M, Jourdain G, Le Coeur S, *et al.* Single-dose perinatal nevirapine plus standard zidovudine to prevent mother-to-child transmission of HIV-1 in Thailand. *N Engl J Med* 2004; **351**:217–228.
4. Adkins JC, Noble S. Efavirenz. *Drugs* 1998; **56**:1055–1064.
5. Staszewski S, Morales-Ramirez J, Tashima KT, *et al.* Efavirenz plus zidovudine and lamivudine, efavirenz plus indinavir, and indinavir plus zidovudine and lamivudine in the treatment of HIV-1 infection in adults. Study 006 Team. *N Engl J Med* 1999; **341**:1865–1873.
6. Lucas GM, Chaisson RE, Moore RD. Comparison of initial combination antiretroviral therapy with a single protease inhibitor, ritonavir and saquinavir, or efavirenz. *AIDS* 2001; **15**:1679–1686.
7. Robbins GK, De Gruttola V, Shafer RW, *et al.* Comparison of sequential three-drug regimens as initial therapy for HIV-1 infection. *N Engl J Med* 2003; **349**:2293–2303.
8. Gulick RM, Ribaudo HJ, Shikuma CM, *et al.* Triple-nucleoside regimens versus efavirenz-containing regimens for the initial treatment of HIV-1 infection. *N Engl J Med* 2004; **350**:1850–1861.
9. Hsiou Y, Ding J, Das K, *et al.* The Lys103Asn mutation of HIV-1 RT: a novel mechanism of drug resistance. *J Mol Biol* 2001; **309**:437–445.
10. Richman DD, ACTG 164/168 Study Team. Loss of nevirapine activity associated with emergence of resistance in clinical trials. *VIII International Conference on AIDS/ III STD World Congress*. 19–24 July 1992, Amsterdam, the Netherlands. Abstract PoB 3576.
11. Richman DD, Shih C-K, Lowy I, *et al.* Human immunodeficiency virus type 1 mutants resistant to nonnucleoside inhibitors of reverse transcriptase arise in tissue culture. *Proc Natl Acad Sci U S A* 1991; **88**:11241–11245.
12. Bacheler L, Jeffrey S, Hanna G, *et al.* Genotypic correlates of phenotypic resistance to efavirenz in virus isolates from patients failing nonnucleoside reverse transcriptase inhibitor therapy. *J Virol* 2001; **75**:4999–5008.
13. Bacheler LT, Anton ED, Kudish P, *et al.* Human immunodeficiency virus type 1 mutations selected in patients failing efavirenz combination therapy. *Antimicrob Agents Chemother* 2000; **44**:2475–2484.
14. Masuda N, Yamamoto O, Fujii M, *et al.* Studies of non-nucleoside HIV-1 reverse transcriptase inhibitors. Part 2: Synthesis and structure-activity relationships of 2-cyano and 2-hydroxy thiazolidenebenzenesulfonamide derivatives. *Bioorg Med Chem* 2005; **13**:949–961.
15. Fujiwara M, Ijichi K, Hanasaki Y, *et al.* Thiadiazole derivatives: highly potent and selective inhibitors of human immunodeficiency virus type 1 (HIV-1) replications *in vitro*. *Microbiol Immunol* 1997; **41**:301–308.
16. Fujiwara M, Kodama EN, Okamoto M, *et al.* Characterization of human immunodeficiency virus type 1 strains resistant to the non-nucleoside reverse transcriptase inhibitor RD4-2217. *Antivir Chem Chemother* 1999; **10**:315–320.
17. Masuda N, Yamamoto O, Fujii M, *et al.* Studies of nonnucleoside HIV-1 reverse transcriptase inhibitors. Part 1: design and synthesis of thiazolidenebenzenesulfonamides. *Bioorg Med Chem* 2004; **12**:6171–6182.
18. Kimpton J, Emerman M. Detection of replication-competent and pseudotyped human immunodeficiency virus with a sensitive cell line on the basis of activation of an integrated beta-galactosidase gene. *J Virol* 1992; **66**:2232–2239.
19. Kodama EI, Kohgo S, Kitano K, *et al.* 4'-Ethynyl nucleoside analogs: potent inhibitors of multidrug-resistant human immunodeficiency virus variants *in vitro*. *Antimicrob Agents Chemother* 2001; **45**:1539–1546.
20. Nameki D, Kodama E, Ikeuchi M, *et al.* Mutations conferring resistance to human immunodeficiency virus type 1 fusion inhibitors are restricted by gp41 and Rev-responsive element functions. *J Virol* 2005; **79**:764–770.
21. Shimura K, Kodama E, Sakagami Y, *et al.* Broad antiretroviral activity and resistance profile of the novel human immunodeficiency virus integrase inhibitor elvitegravir (JTK-303/GS-9137). *J Virol* 2008; **82**:764–774.
22. Jones G, Willett P, Glen RC. Molecular recognition of receptor sites using a genetic algorithm with a description of desolvation. *J Mol Biol* 1995; **245**:43–53.
23. Berman HM, Westbrook J, Feng Z, *et al.* The Protein Data Bank. *Nucleic Acids Res* 2000; **28**:235–242.
24. Protein data base, NCBI Structure. (Accessed 27 May 2008.) Available from http://www.ncbi.nlm.nih.gov/Structure/
25. Ren J, Milton J, Weaver KL, Short SA, Stuart DI, Stammers DK. Structural basis for the resilience of efavirenz (DMP-266) to drug resistance mutations in HIV-1 reverse transcriptase. *Structure Fold Des* 2000; **8**:1089–1094.
26. Allen FH. The Cambridge Structural Database: a quarter of a million crystal structures and rising. *Acta Crystallogr B* 2002; **58**:380–388.
27. Kantor R, Machekano R, Gonzales MJ, Dupnik K, Schapiro JM, Shafer RW. Human Immunodeficiency Virus Reverse Transcriptase and Protease Sequence Database: an expanded data model integrating natural language text and sequence analysis programs. *Nucleic Acids Res* 2001; **29**:296–299.
28. Shafer RW. Stanford HIV Drug Resistance Database, NNRTI Resistance notes. (Accessed 27 May 2008.) Available from http://hivdb.stanford.edu/cgi-bin/NNRTIResiNote.cgi 2008
29. Clark SA, Calef C, Mellors JW. Mutations in retroviral genes associated with drug resistance. In *HIV Sequence Compendium 2005*. Edited by T Leitner, B Hahn, P Marx, F McCutchan, J Mellors, S Wolinsky & B Korber. New Mexico: Los Alamos National Laboratory 2005; pp. 80–174.
30. Parikh U, Calef C, Clark SA, Mellors JW. Mutations in retroviral genes associated with drug resistance. In *HIV Sequence Compendium 2003*. Edited by T Leitner, B Hahn, P Marx, F McCutchan, J Mellors, S Wolinsky & B Korber. New Mexico: Los Alamos National Laboratory 2003; pp. 38–122.
31. Balzarini J, Kleim JP, Riess G, Camarasa MJ, De Clercq E, Karlsson A. Sensitivity of (138 Glu->Lys) mutated human immunodeficiency virus type 1 (HIV-1) reverse transcriptase (RT) to HIV-1-specific RT inhibitors. *Biochem Biophys Res Commun* 1994; **201**:1305–1312.
32. Schinazi RF, Larder BA, Mellors JW. Mutations in retroviral genes associated with drug resistance: 1999–2000 update. *Int Antiviral News* 1999; **7**:46–69.
33. Ding J, Das K, Moereels H, *et al.* Structure of HIV-1 RT/ TIBO R 86183 complex reveals similarity in the binding of diverse nonnucleoside inhibitors. *Nat Struct Biol* 1995; **2**:407–415.
34. Ren J, Esnouf R, Garman E, *et al.* High resolution structures of HIV-1 RT from four RT-inhibitor complexes. *Nat Struct Biol* 1995; **2**:293–302.
35. Smerdon SJ, Jager J, Wang J, *et al.* Structure of the binding site for nonnucleoside inhibitors of the reverse transcriptase of human immunodeficiency virus type 1. *Proc Natl Acad Sci U S A* 1994; **91**:3911–3915.
36. Kohlstaedt LA, Wang J, Friedman JM, Rice PA, Steitz TA. Crystal structure at 3.5 A resolution of HIV-1 reverse transcriptase complexed with an inhibitor. *Science* 1992; **256**:1783–1790.